

FAST AND INEXPENSIVE DETECTION OF  
BACTERIAL VIABILITY AND DRUG  
SUSCEPTIBILITY THROUGH METABOLIC  
MONITORING

FAST AND INEXPENSIVE DETECTION OF BACTERIAL  
VIABILITY AND DRUG RESISTANCE THROUGH  
METABOLIC MONITORING

By

SONDOS AYYASH, B.ENG.

B. Eng. (Ryerson University, Toronto, Ontario)

A Thesis

Submitted to the School of Graduate Studies

In Partial Fulfillment of the Requirements

For the Degree

Master of Applied Science

McMaster University

© Copyright by Sondos Ayyash, August 2016

MASTER OF APPLIED SCIENCE (2016)

McMaster University

(Biomedical Engineering)

Hamilton, Ontario, Canada

TITLE

FAST AND INEXPENSIVE DETECTION OF BACTERIAL  
VIABILITY AND DRUG RESISTANCE THROUGH  
METABOLIC MONITORING

AUTHOR

SONDOS AYYASH, B.Eng.

SUPERVISOR

Professor P. R. Selvaganapathy, Associate Professor

Department of Mechanical Engineering

NUMBER OF PAGES

CIII, 103

# Abstract

Conventional methods for the detection of bacterial infection such as DNA or immunoassays are either expensive, time consuming, or not definitive; thus may not provide all the information sought by the medical professionals. In particular, it is difficult to obtain information about viability or drug effectiveness, which are crucial to formulate a treatment. Bacterial culture test is the “gold standard” because it is inexpensive and does not require extensive sample preparation, and most importantly, provides all the necessary information sought by healthcare professionals, such as bacterial presence, viability and drug effectiveness. These conventional culture methods, however, have a long turnaround time: anywhere between 1 day to 4 weeks. This thesis proposes to solve this problem by monitoring the growth of bacteria in thousands of nanowells simultaneously to identify its presence in the sample and its viability, faster. The segmentation of a sample with low bacterial concentration into thousands of nanoliter wells digitizes the samples and increases the effective concentration in those wells that contain bacteria. The user may then monitor the metabolism of the aerobic bacteria by using an oxygen sensitive fluorophore, ruthenium tris (2,2'-dipyridyl) dichloride hexahydrate ( $\text{Ru}(\text{Bpy})_3$ ) by monitoring the dissolved oxygen concentration in the nanowells. Using E.Coli K12, it is demonstrated that the detection time of E.coli can be



as fast as 35-60 minutes with sample concentrations varying from  $10^4$  (62 minutes for detection),  $10^6$  (42 minutes) and  $10^8$  cells/mL (38 minutes). More importantly, throughout the thesis it is also demonstrated that reducing the well size can reduce the time of detection. Finally, this thesis will discuss how the drug effectiveness information can be obtained in this format by loading the wells with the drug and monitoring the metabolism of the bacteria. The method that is developed in this thesis is low cost, simple, requires minimal sample preparation and can potentially be used with a wide variety of samples in resource poor setting to detect bacterial infections such as Tuberculosis.

# Acknowledgement

I wish to express my gratitude to my supervisor, Professor Ponnambalam Ravi Selvaganapathy for his aid and guidance throughout my time as his student. Not only has he been a great mentor but also he has given me the opportunity to attend conferences and competitions, where I was able to meet so many interesting people and develop as an individual through these many experiences.

Additionally, completing my masters would have been all the more difficult were it not for the support and friendship provided by my CAMEF team members.

I would especially like to thank my amazing siblings for the love, support, and constant encouragement I have gotten over the years, because I undoubtedly could not have done this without them.

Lastly, to my parents, you are my rock! You have never wavered in your love and support. I owe everything to you. Thank you for teaching me what it means to never give up, and to always challenge myself to do more. You have been a constant source of encouragement and enthusiasm, along this journey in allowing me to realize my own potential. Love you!

# Table of Contents

Abstract .....	ii
Acknowledgement .....	iv
Table of Contents .....	v
List of Figures .....	ix
List of Tables .....	xii
Chapter 1 .....	1
Motivation and Organization .....	1
1.1 Motivation.....	1
1.2 Organization of the Chapters .....	4
1.3 Contributions.....	5
Chapter 2 .....	6
Introduction.....	6
2.1 Bacterial Disease.....	6
2.2 Physical and Morphological Characteristics of Bacteria .....	7
2.1.2 Outer Cell Structure: Cell Membrane and Cell Wall.....	8
2.1.2 Growth Phases of Bacteria.....	11
2.1.2 Categories of Bacterial Metabolism.....	13
2.2 Conventional Diagnostic Techniques .....	15

2.3 Non-Molecular Laboratory Diagnostic Methods .....	17
2.3.1 Staining .....	17
2.3.2 Agar Culture.....	19
2.3.3 Liquid Culture .....	23
2.3.4 Drug Susceptibility .....	25
2.4 Molecular Based Detection.....	28
2.4.1 Immunoassays.....	28
2.4.2 Nucleic acid based technologies .....	31
2.6 Summary .....	36
Chapter 3 .....	37
Device Design, Working Principle, and Fabrication .....	37
3.1 Device Design and Working Principle.....	38
3.1.1 Design Criteria .....	40
3.1.2 Device Design .....	41
3.2 Working Principle.....	42
3.3 Materials and Methods.....	45
3.3.1 Materials.....	45

3.4 Sample Preparation.....	51
3.5 Sample Loading and Experimental Setup.....	58
3.6 Summary .....	60
Chapter 4.....	61
Results and Discussion.....	61
4.1 Sample dispensing.....	61
4.2 Distribution of bacteria .....	70
4.3 Demonstration of metabolic monitoring of bacterial growth.....	72
4.4 Bacterial Viability.....	78
4.5 Fluorescence response and bacterial metabolism .....	80
4.6 Drug susceptibility .....	82
4.7 Nanowell Shape and Size.....	84
4.8 Summary.....	85
Chapter 5.....	87
Contributions and Future Work .....	87
5.1 Contributions.....	87
5.2 Future Work.....	89
Reference: .....	93

Appendix A: .....	99
Device Fabrication .....	99
Appendix B: .....	102
Measuring Mean Grey Value .....	102
Appendix C: .....	102
Inoculation of a Petri dish containing agar .....	102

# List of Figures

Figure 1. Global Infectious Disease Deaths, by Region, 2004.

Figure 2. Diagram of cell types. a: prokaryotic, b: eukaryotic.

Figure 3. Gram Staining Process

Figure 4: Bacteria Cell Structures (a) Gram Positive (b) Gram Negative

Figure 5. Standard bacterial growth curve and growth phases of *E. coli* in liquid culture.

Figure 6. Laboratory procedures used in confirming a clinical diagnosis of infectious disease with a bacterial etiology

Figure 7. Ziehl-Neelsen staining of mycobacteria tuberculosis

Figure 8. Solid culturing can differentiate between bacterial species in a sample

Figure 9. Bacterial colony morphology

Figure 10. Antibiotic sensitivity test with thin wafers.

Figure 11. Broth microdilution test

Figure 12: Common ELISA formats. In the assay, the antigen of interest is immobilized by direct adsorption to the assay plate or by first attaching a capture antibody to the plate surface. Detection of the antigen can then be performed using an enzyme-conjugated primary antibody (direct detection) or a matched set of unlabeled primary and conjugated secondary antibodies (indirect detection).

Figure 13: Schematic of PCR. Each cycle of the PCR includes heat denaturation of the double stranded DNA template into single strands, annealing of an oligonucleotide primer complementary to sequence being amplified, and extension of the annealed primer using a thermostable DNA polymerase and nucleotide triphosphates. Repeated cycles result in exponential, sequence specific amplification of the original target.

Figure 14: Miniaturization and compartmentalization of a milliliter volume into several microliter volumes. The concentration of bacteria (red triangles) is small in the large volume. However, the concentration is high in some of the microvolumes while is zero in others.

Figure 15: Loading of solution and sealing for imaging procedure

Figure 16. The flow process of the device fabrication. 1) silicon wafer is cleaned and prepared for use 2) 100 $\mu$ m thickness of SU8 is deposited on the surface of the silicon wafer 3) It is then soft-baked so that the su8 layer is densified 4) alignment and exposure for patterning of the first SU8 layer. 5) Post-exposure bake is done to reduce the standing wave effect 6) Next, Development is used to control development uniformity and Etch. 7) Postbake, hardbake used to stabilize and harden the photoresist. 8) Next, these patterns are transferred into the substrate through etching. 9) Lastly, after the wafer has been etched, the remaining photoresist must be removed.

Figure 17: Fabrication process of nanowell array

Figure 18. Filling a solution 1.5  $\mu$ L of methylene blue with DI water into nanowell array using a back and forth motion. Each nanowell is 100x100x100  $\mu$ m in dimension and holds 1nL.

Figure 19. Percentage of Nanowells filled per swipe (with a coverslip) using a mixed solution of de-ionized water and methylene blue.

Figure 20. Percentage of wells filled with each swipe, of a 1nL array, with solutions of different viscosities: DI water (0.001pa-s), milk (0.003pa-s), xantham gum (non-Newtonian fluid), and artificial sputum (0.4pa-s).

Figure 21. Confocal microcopy imaging was used to capture a 1 nL well volume. Fluorescence of the oxygen quenching fluorophore Ru(BPY)<sub>3</sub> is imaged. The image on the left is at time=30min and figure on the right is time =2 hrs at a concentration of 10<sup>9</sup>CFU/mL.

Figure 22. Controls. Fluorescence behavior when O<sub>2</sub> gas bubbled in solution ([O<sub>2</sub>] = 15.6 mg/l), at atmospheric conditions ([O<sub>2</sub>] = 6 mg/l), and when oxygen scavenger is added ([O<sub>2</sub>] = 0 mg/l) respectively. *Fluorescence intensities were normalized (to t=0) to allow direct comparison of fluorescent increases/decreases.*

Figure 23. The growth of GFP-expressing E. coli K12 in LB media is demonstrated within a 1nL nanowell at image on left, t=0 and image on right, t=12hrs.

Figure 24. Different Concentrations of bacteria were imaged for metabolic rates of detection. *Fluorescence intensities were normalized (to t=0) to allow direct comparison of fluorescent increases.*



Figure 25. Confocal microscopy is used to image the fluorescent intensity of the RU(BPY)3 when a drug (ampicillin) is added to the nanowell, it inhibits bacterial growth, whereas when no drug is present in the well, the e coli OP50 strain grows naturally and it can be observed that an increase in fluorescence occurs due to oxygen quenching. *Fluorescence intensities were normalized (to  $t=1$ ) to allow direct comparison of fluorescent increases/decreases.*

Figure 26. The volume size of the nanowell effects the results significantly. The smaller the well volume (100nL, 1nL), the more prominent the changes in oxygen levels within the well. The larger the well, the longer the time it takes to detect changes in oxygen levels (0.1mL). *Fluorescence intensities were normalized (to  $t=0$ ) to allow direct comparison of fluorescent increases.*

## List of Tables

Table 1. Summary of advantages and limitations of each rapid detection [1]

# Chapter 1.

## Motivation and Organization

### 1.1 Motivation

Infectious diseases caused by protozoa, bacteria, fungi and viruses, are a leading cause of global human suffering. According to World health Organization (WHO), infectious diseases claim 16.7 million lives worldwide each year[2]. Bacterial infectious diseases are responsible for a significant portion of these deaths. Annually, an estimated 16% of all deaths worldwide result from infectious diseases [3], disproportionately afflicting the developing world. For instance, Tuberculosis, caused by the bacteria *Mycobacterium tuberculosis*, is the top infectious disease killer worldwide [4], and accounts for 1.5 million deaths worldwide, as shown in figure 1 [4].

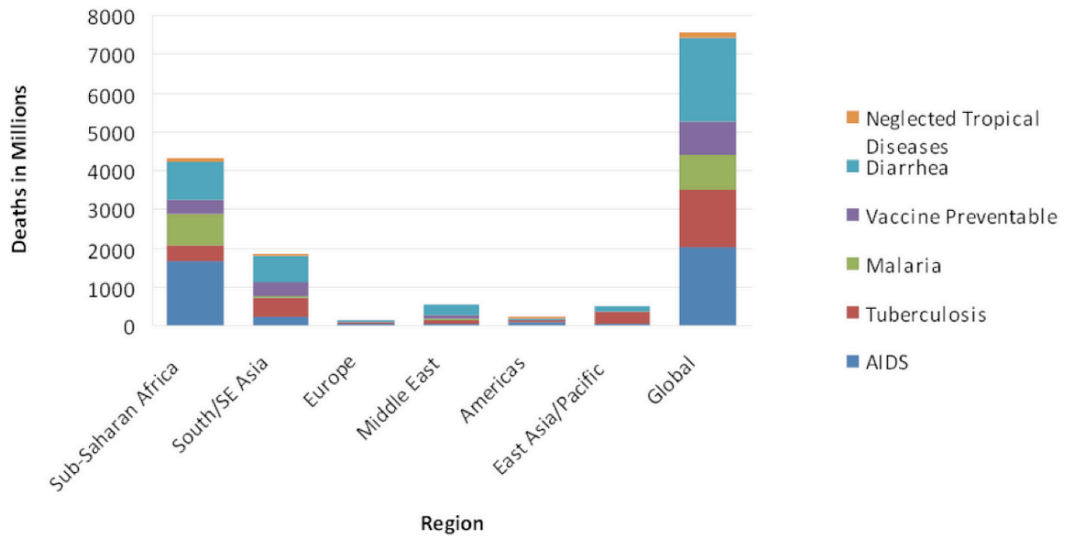


**Figure 1.** Global Infectious Disease Deaths, by Region, 2004. Reproduced from [2].

Despite being curable, global morbidity and mortality rates of these diseases remain high [5]. The bottleneck in the management of infectious disease is not in poor treatment but in the proper and early detection of the disease [6]. Additionally, treatment for many of these bacterial infections is inexpensive, but its diagnosis and identification of a suitable treatment is costly. As a result, there still remains a high rate of bacterial infection-related deaths worldwide. This is an issue because, WHO reports that the majority of deaths caused by infectious diseases occur in low- and middle- income countries where cost is an important factor[7]. Thus, the development of an inexpensive point of care (POC) diagnostic technique to quickly and accurately identify a suitable treatment for the infected persons is key to reducing the number of cases of reported

deaths caused by bacterial infectious diseases in resource poor settings and preventing the spread of disease.

Current diagnostics such as immunoassay or nucleic-based detection methods are unable to provide all information sought by healthcare professionals. Examples of these diagnostic tools are ELISA and PCR. For instance, ELISA is not able to determine the viability of the bacteria in a sample. It is costly and requires skilled laboratory technicians to operate the device. Also, immunoassays such as PCR are also unable to determine the viability of bacteria, require expensive reagents and require complex instrumentation to operate. As a result, healthcare professionals often order multiple tests serially in the face of inconclusive evidence.

Then there is the bacterial culture test. Bacterial culture involves taking a swab from a patient that appears to have a bacterial infection. The sample is then deposited onto a selective and/or differential media in which a wide the bacteria of interest is cultured. However, the culture test provides all the information sought by healthcare professionals including presence, viability and drug susceptibility of the bacteria. For this reason it is considered the ‘gold standard’. However, it is also the method that takes the longest; turnaround times can range from 12 hours to several weeks. Therefore, this thesis focuses on developing a nanowell array, which allows the rapid and inexpensive detection of bacterial presence, viability and susceptibility to drugs.

## **1.2 Organization of the Chapters**

The thesis is organized in the following chapters:

Chapter 2 presents an introduction to bacterial infectious diseases followed by current diagnostic devices that already exist. Then, a comparison of the methods that are currently used, the advantages and disadvantages that comes with each.

Chapter 3 establishes the proposed design and describes the advantages of this design over other already existing diagnostic devices available in the literature. It details the functionality and operation of the device, and its potential for fast inexpensive detection. It determines the critical dimensions of the design and details some of the experiments that were performed to determine certain crucial design parameters. The fabrication techniques and materials used in the micro-fabrication, the setup and operation of the device are also discussed within this chapter.

Chapter 4 describes the experimental setup and the characterization of the device and presents the results obtained from the device. It specifies the characterization of the device and the filling of the wells. The chapter ends with the results, and demonstrates the proposed diagnostic device as the solution to the problem presented in the first chapter.

Chapter 5 ends this thesis by highlighting the contributions of the research and then provides a number of suggestions for the future development of the device.

### **1.3 Contributions**

The main contributions for this research are listed below.

-Recently, there have been many developments in diagnostic devices for the detection of infectious diseases, especially molecular diagnostics. However, none of them were able to provide all the information sought by healthcare professionals with fast turnaround times. This thesis discusses the integration of the culture test with miniaturization and metabolic monitoring of the bacteria using fluorescence signal analysis. The device developed in this thesis represents the first nanowell array device based on culture principles that is able to diagnose presence of bacterial infections, viability and drug susceptibility with fast turnaround times in comparison to the conventional method.

-In this thesis, characterization of the filling is achieved so that the inside of the nanowells are hydrophilic and the outer surface is hydrophobic to allow filling of wells to happen with ease.

-The thesis demonstrates repeatability and reliability of the device in identifying the bacterial viability rapidly and the identification of drug effectiveness.

## **Chapter 2.**

### **Introduction**

#### **2.1 Bacterial Disease**

Bacterial diseases remain an important global problem in public health, and has been recognized as a leading cause of morbidity and mortality, especially in developing countries[2]. According to World Health Organization, infectious diseases account for 20% of deaths worldwide. Pathogenic bacteria have many different means of transmission, which includes those that are: foodborne, airborne, or waterborne [8]. For instance, Acinetobacter, Campylobacter and Enterobacteriaceae are some of the leading causes of bacterial infectious diseases worldwide[9]. Antibiotics can fight and prevent diseases caused by bacteria. However, when bacteria resist the effect of an antibiotic, it becomes drug resistant. Poverty, poor access to healthcare and antibiotic resistance are instrumental in cultivating conditions that allow disease to spread[10]. Prevention and treatment of bacterial disease has become critical to avoid re-emergence of these pathogens.



## 2.2 Physical and Morphological Characteristics of Bacteria

Organisms can be distinguished into two major groups based on their structure: prokaryotes and eukaryotes. Most cells belong to the eukaryote category. When a membrane encloses the nucleus, and the nuclear material does not mix with the cytoplasm, it is categorized as eukaryotic, demonstrated in figure 2b. Prokaryotes on the other hand, do not have a nuclear membrane and the nuclear material is present in the cytoplasm, as shown in figure 2a. As such, all bacteria are considered to be prokaryotes.

[11]

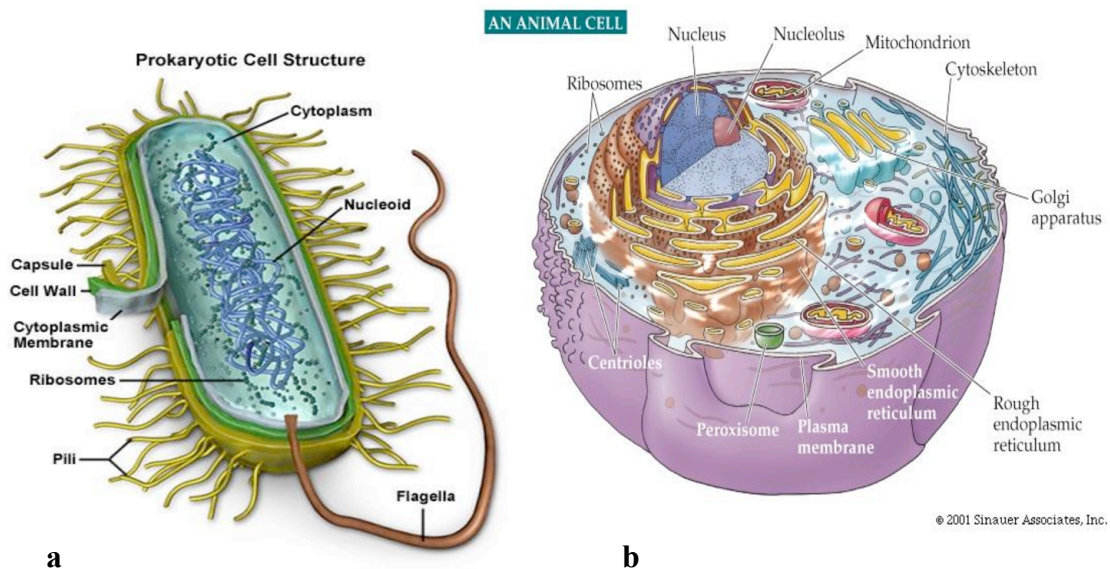


**Figure 2.** Diagram of cell types. a: prokaryotic, b: eukaryotic. Reproduced from [12].

### **2.1.2 Outer Cell Structure: Cell Membrane and Cell Wall**

Bacteria can be categorized into one of two broad categories as a result of the gram stain test: gram-positive and gram-negative. The gram stain is the primary step for the identification of bacteria. Gram-positive bacteria appear purple whereas gram-negative bacteria appear red, which is a result of the biochemical and structural differences of the cell wall.

Peptidoglycan makes up as much as ninety percent of the thick cell wall (15-80 nm) enclosing the plasma membrane in Gram-positive bacteria. Peptidoglycan serves many purposes, namely, gives the bacterial cell shape, and provides a protection from the environment. The multiple layers of peptidoglycan retain the purple crystal violet (figure 3). A decolourizing agent such as ethanol or acetone is then added and the cell wall is dehydrated, in which the stain-iodine complex is trapped and the cell appears to be purple. Teichoic acids, acidic anionic polysaccharides, are anchored to the plasma membrane in gram-positive bacteria and are at right angles to the layers of peptidoglycan. Teichoic acids give the cell wall a negative charge and function as a chelating agent [13].

The cell wall of the gram-negative bacteria however, is very different than that of the gram-positive bacteria. The peptidoglycan layer (2nm thickness) makes up only ten percent of the cell wall, which is sandwiched between an inner cytoplasmic cell membrane and a bacterial outer membrane. The space between the cytoplasmic

membrane and the outer membrane is called the periplasmic space and it is an important location for Gram-negative bacteria to perform many chemical reactions. In addition, due to the thin layer of the peptidoglycan, when the bacteria is exposed to the decolorizing agent during the gram staining process, it is not able to retain the color (figure 3).

Additionally, the cell wall of gram-negative bacteria contains an outer membrane composed of phospholipids and lipopolysaccharides. The gram negative bacteria are not able to retain the crystal violet but are able to retain the counterstain, which happens to be red in color[13].

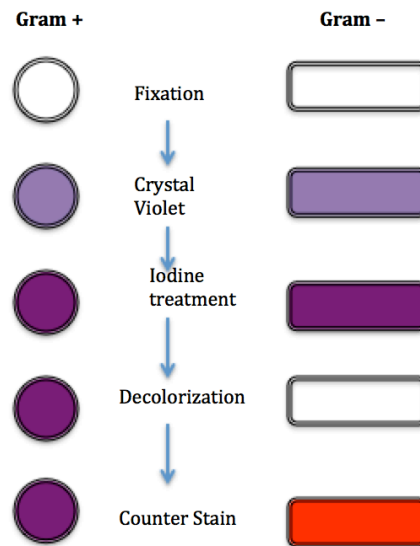


**Figure 3.** Gram Staining Process.

Gram-negative bacteria typically has a cell wall with a thickness of 4nm, as shown in figure 4 [14]. *E.coli*, a gram-negative bacterium, has a cell wall that consists of fimbriae and a cell wall with an outer membrane consisting of lipopolysaccharides, periplasmic space, peptidoglycan layer, and a cytoplasmic membrane. Gram-positive bacteria typically have a thicker peptidoglycan layer than gram-negative bacteria, as demonstrated in figure 4. An example of pathogenic gram-positive bacteria is *Streptococcus*.

There are classes of bacteria that do not share the characteristics of gram positive or negative bacteria. These include the family of *Chlamydiaceae* and *Mycoplasmataceae*. An example of this is *Mycobacterium*. *Mycobacterium* is a genus of actinobacteria, in which the bacteria has a cell envelope, which is not typical of gram positives or gram negatives. The mycobacterial cell envelope does not have an outer membrane typical of gram-negative bacteria. Instead, it has an outer membrane made of mycolic acids in addition to the peptidoglycan layer in their cell wall. Mycolic acids are unique to mycobacterium and its waxy surface acts to resist staining. In addition, nutrients pass through it very slowly due to the outer mycolic acid layer, which in turn causes very slow growth times for bacteria in culture[13]. Thus, because the cell wall is resistant to water-based stains, these organisms require a staining technique known as “acid-fast”, which involves heat to melt the wax (mycolic acid) and allow the stain to move into the cell

wall. The combination of carbol-fuchsin, a strong stain, and heat, forces the stain through the cell wall. Once the bacterium is cooled, it becomes resistant to decolourization.

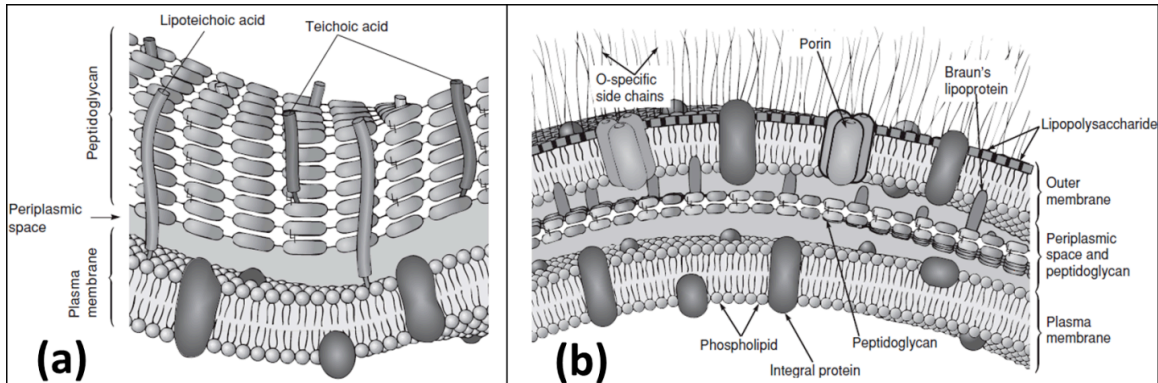


**Figure 4:** Bacteria Cell Structures (a) Gram Positive (b) Gram Negative. Reproduced from [15]

### 2.1.2 Growth Phases of Bacteria

In order to study and diagnose bacteria efficiently it is important to understand the growth and metabolic behaviour at different stages of the cell cycle. The growth curve of each species of bacteria can help microbiologists know which phase it is in at different time points. Growth of a bacterial population can be illustrated using a bacterial growth curve shown in figure 5. Bacterial growth curves have four main phases: lag, log, stationary and death[16]. When a bacterial colony is picked up from an agar plate and onto a fresh liquid medium, the bacteria are typically dormant[16]. As time progresses in the lag phase, the bacteria switch to an actively growing state. A horizontal line at the start of the growth curve represents the lag phase and can last from less than an hour to

days depending on various factors such as temperature, species of bacteria, or if the bacteria is 'shocked'. During the lag phase, bacteria are maturing and not able to divide yet, however metabolic processes occur during this time (i.e. enzyme production, and waste products)[16]. Bacteria then enter into an exponential phase, also known as the log phase whereby bacteria proliferate rapidly through binary fission. This phase is characterized by cell doubling[17]. Depending on the species of bacteria, the doubling time can range from 20 minutes (*E.coli*) to 14 days (*M. Leprae*). The slope of the line in the growth curve represents the rate of cell growth (number of cell divisions per unit time). In the case of pathogenic bacteria, it is during the log phase that disease symptoms appear. After several hours of rapid cell division there will be a depletion of nutrients in the medium and a build-up of toxic products[17]. Therefore, the cell division can't continue at the same rate, and so the growth phase tapers off. This is known as the stationary phase. During this phase, the cell growth rate and cell death rate are equal, which is represented by a horizontal line[16]. When toxin concentrations are high and complete exhaustion of nutrients occurs, the bacteria enter the death phase[17]. This phase involves the decline in bacterial population, which means that the rate of cell death will be highest at this time. This is key to understanding the characteristics of the growth and metabolism during each phase as time progresses.

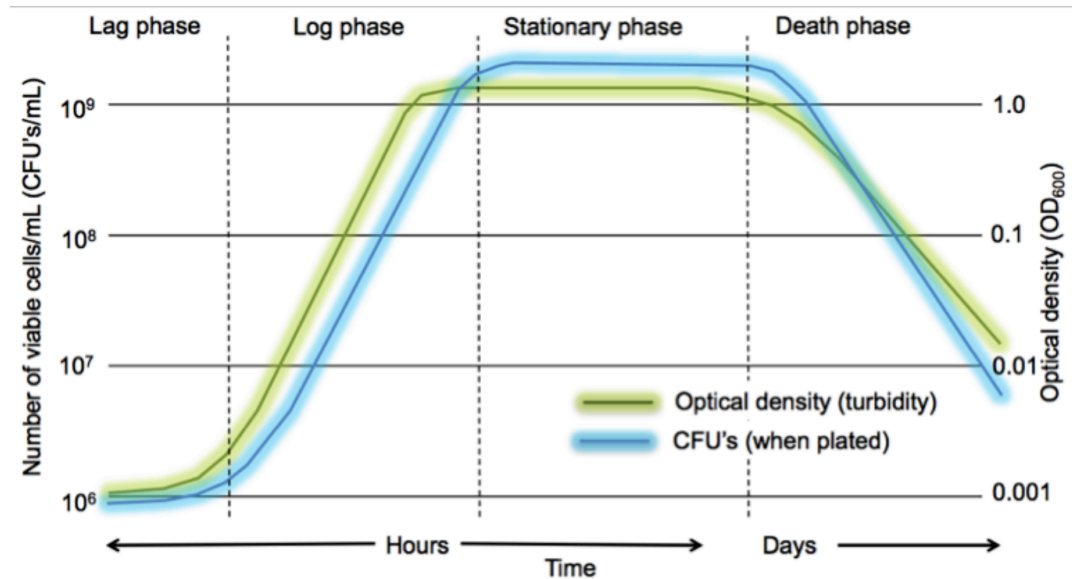


**Figure 5.** Standard bacterial growth curve and growth phases of *E.coli* in liquid culture. Reproduced from [18].

### 2.1.2 Categories of Bacterial Metabolism

Metabolism plays an important role in our bacterial detection device. It refers to all of the metabolic reactions (chemical reactions) that occur within a living cell, and the production of energy and the synthesis of new molecules. With diversity in metabolism, bacteria can be categorized according to three principles: the kind of energy used for growth, the carbon source, and the electron donors used for growth [19]. The first classification of the metabolism is based on how the microorganism obtains carbon for synthesizing cell mass. Autotrophs are microorganisms that use only inorganic nutrients

(CO<sub>2</sub>) as their source of energy whereas heterotrophs require organic carbon sources[20]. The second classification of metabolism relies on how the microorganism obtains reducing equivalents in biosynthetic reactions. Organotrophic microorganisms can obtain reducing equivalents from inorganic compounds, while organotrophic microbes obtain reducing equivalents from organic compounds instead[19]. Another way to categorize bacteria is based on their characteristic energy source. There are various energy sources available that microorganisms can use for metabolism. In order to produce ATP, depending on the species of bacteria, nutrients can come from different energy sources. Microorganisms that rely on light as their source of energy are called phototrophs [19]. Alternatively, organisms that use organic or inorganic chemicals as the source of energy are referred to as chemotrophs [19]. These three characteristic groups can be combined differently to describe the metabolic properties of the microbe. For instance, *E.coli* is used throughout our experiments is a chemo-organo-heterotroph. A chemo-organo-heterotrophic organism is one that requires organic substrates to get its carbon for growth and development, and that produces its energy from oxido-reduction of an organic compound [21].

Identifying the classification of a microorganisms based on their metabolism is important. It identifies the type of bacterial fermentation and the by-products that are



produced. This acts as a characteristic biochemical “fingerprint” of a bacterial species to help the user select the appropriate metabolite to monitor.

## **2.2 Conventional Diagnostic Techniques**

There are two main categories of bacterial detection: molecular diagnostics (figure 6) and non-molecular diagnostic methods (figure 6). Molecular diagnostics are techniques that are frequently used to diagnose diseases based on the presence and quantity of specific biomolecules, such as deoxyribonucleic acid (DNA), ribonucleic acid (RNA), protein or metabolites. Non-molecular diagnosis methods of bacterial diseases include techniques such as microscopy and culturing methods. Descriptions of the most commonly used conventional detection methods are provided in the next section.

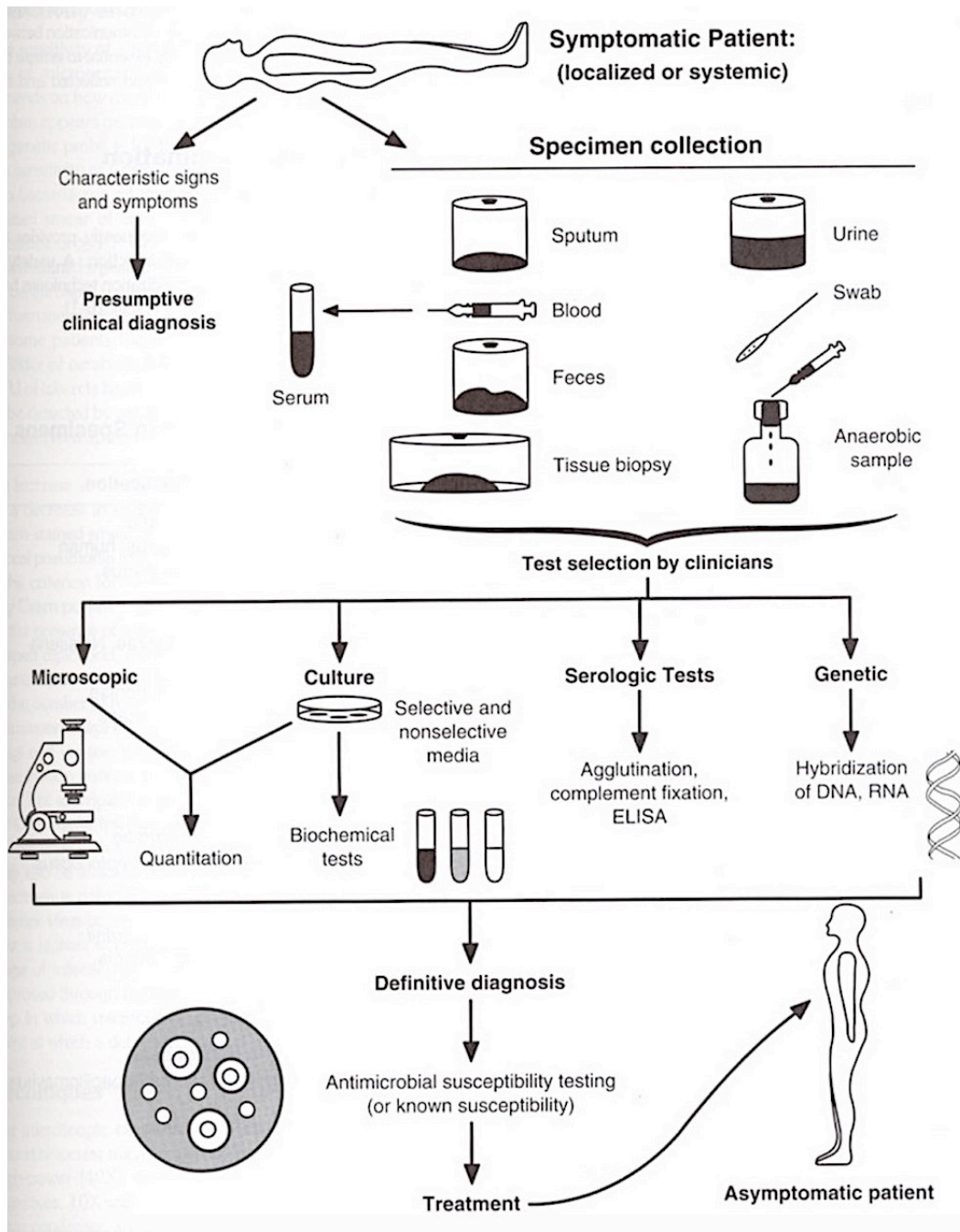


**Figure 6.** Laboratory procedures used in confirming a clinical diagnosis of infectious disease with a bacterial etiology. Reproduced from [22].

## **2.3 Non-Molecular Laboratory Diagnostic Methods**

### **2.3.1 Staining**

AFB Staining is done to identify active bacterial infections. As mentioned previously, bacteria such as *E.coli* can be identified using the gram stain. However, not all bacteria can be identified using a gram stain. There are some bacteria that are impermeable to ordinary stains such as the gram stain (due to high levels of mycolic acid within their cell wall) and are stained with carbol fuchsin combined with phenol instead [23]. This is known as the Ziel-Neelsen method. In the Ziehl-Neelsen (ZN) method, commonly referred to as the ‘hot’ technique, the phenol-carbol fuchsin stain is heated to allow the dye to penetrate the waxy mycobacterial cell wall[24]. Whereas, in the Kinyoun Method known as the ‘cold’ technique, increasing the concentration of basic fuchsin and phenol, as well as incorporating a ‘wetting agent’ chemical can achieve penetration of the cell wall for staining[23].

The principle behind staining involves the binding of the stain to the mycolic acid (lipid layer) in the cell wall of the mycobacteria[24]. After staining, an acid decolorizing solution is applied, which removes the red dye from the surrounding cells and tissues, but not from mycobacteria. Mycobacteria will instead retain (hold fast) the dye, which subsequently appears as a red color[24]. Once decolorization is accomplished, the smear

is counterstained with either methylene blue or malachite green, which dyes the background. This serves as a contrast color against the red acid-fast bacteria, to visualize it better, as shown in figure 7.

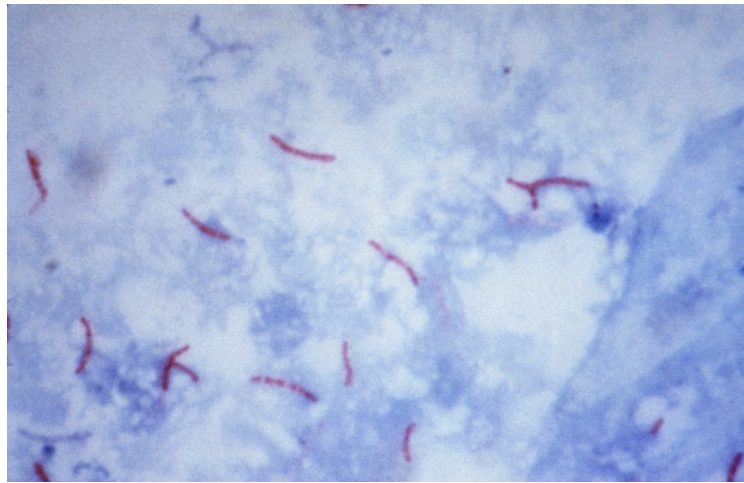


**Figure 7.** Ziehl-Neelsen staining of *mycobacteria tuberculosis*. Produced from [25].

Staining techniques are one of the oldest, most rapid, inexpensive and simplest methods that exist. However, there are some disadvantages that are associated with them. Firstly, the acid-fast method cannot distinguish between viable and dead organisms. Thus, upon follow up of treatment, the smear may be positive, yet the culture is negative. In addition, one of the most limiting factors is the low sensitivity of this method[26], ZN staining fails to identify mycobacteria in numbers less than  $10^5$  cells/mL[27], which can be a problem when detecting low levels of bacteria in a sample. Lastly, acid fast has

limited specificity, because all mycobacteria are acid fast (have similar cell wall properties). It can identify a genus of bacteria, but not the species[28]; therefore it requires more specific testing.

Therefore, a positive AFB can only taken as an indicator for more comprehensive testing. Interpretations of microscopy results are then confirmed through culturing methods.

### **2.3.2 Agar Culture**

The culture test is considered the ‘gold standard’ for the detection of bacterial infections because it provides all the information sought by healthcare professionals. A definitive diagnosis of a bacterial infection can only be done with the culture test[29]. A culture test involves collecting a sample of fluid from the patient and then evaluating it in a laboratory to detect infections and determine their susceptibility to various antibiotics.

Culturing is a technique that is used to study bacteria on a media that contains nutrients; this may be a solid media or liquid media[30]. Liquid culture differs from solid culture in that liquid media is planktonic, which means that it permits bacterial cells to move freely throughout the medium[30]. This makes it difficult to identify the presence of different species of bacteria in the sample. To effectively study bacteria in liquid culture, one must inoculate the medium from a known pure culture such as a single colony on a solid medium[30]. This insures that the liquid culture is a pure culture.

Alternatively, with solid media, culturable cells will proliferate in the spot where the bacteria were deposited[30]. This is advantageous because it gives doctors an opportunity to isolate pure cultures and study their morphology. In order to isolate a specific type of bacteria from a mixture of other bacteria, a solid media is used rather than a liquid media (as shown in figure 8)[30]. However, it is important to choose a selective growth media that ensures the proliferation of bacteria that is being testing for and inhibit growth of unwanted bacteria.

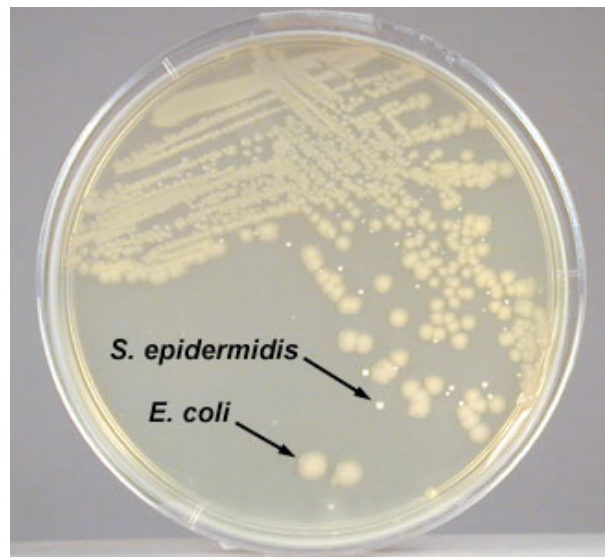


**Figure 8.** Solid culturing can differentiate between bacterial species in a sample. Reproduced from [31].

Streaking the sample across an agar plate and incubating it for a period of time to allow bacteria to multiply till visible colonies form (a colony generally contain more than  $10^7$  organisms) is the principle behind the culture test[32]. Bacterial culture streaking

methods are used to identify microorganisms and to diagnose infection[32]. Culturing is performed to confirm the type of infection and assist with the best choice of antibiotic. In addition, information on the viability of the microorganism is determined with culture[32]. If the specific species of bacteria divide on the surface to form colonies it is viable, if not it is dead.

Bacteria are grown on selective culture media to inhibit the growth of contaminants and encourage the growth of desired bacteria. When a mixed culture is grown on a plate, one can recognize different species of bacteria based on their colonial characteristics. Each bacterial species has its own colony morphology which can be used to identify different species of bacteria based on these characteristics. There are some common colony types that can be identified based on visual observation. These categories of identification include form, size, surface, texture, color, elevation and margin (shown in figure 9).

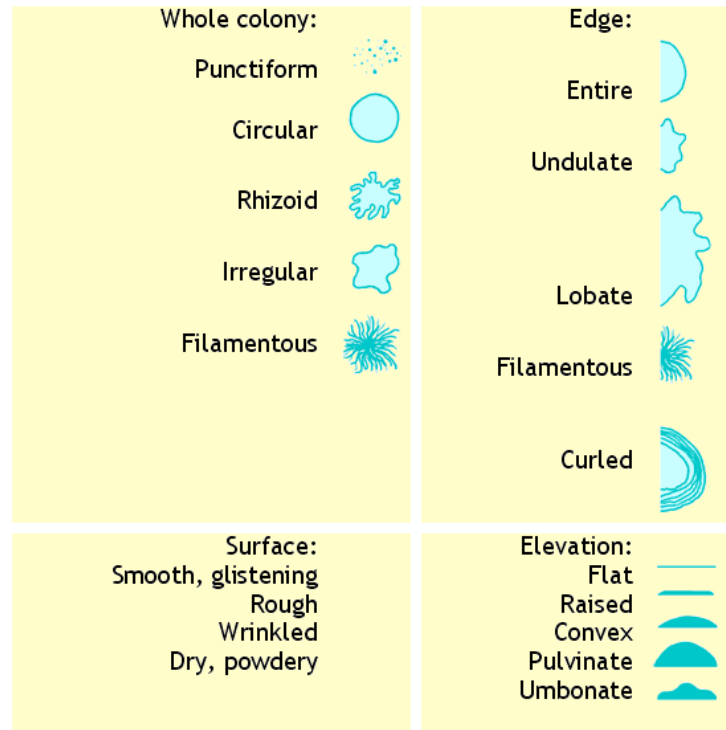


**Figure 9.** Bacterial colony morphology. Reproduced from [33].

However, this method has a disadvantage in that, slow-growing bacteria such as *mycobacteria tuberculosis*, can take 3-4 weeks (sometimes longer) for result and an additional 4-6 weeks to determine drug susceptibility[34]. Although culture for TB is more sensitive than staining, it still needs  $10^1$ - $10^2$  bacilli/ml for the diagnostic yield[27].



### 2.3.3 Liquid Culture

Bacteria can be grown on solid media but can also be grown in liquid media as well. Liquid broth can be selective or non-selective, similar to that of solid media. An indicator of the presence and proliferation of the bacteria, the liquid media becomes clouded. Liquid culture has the advantage that it has a higher sensitivity than solid culture, meaning that it growing low concentrations of bacteria is ideal for this method[35]. But a disadvantage is that it may be difficult to differentiate between different bacterial colonies within the solution, since they are all mixed[35].

Liquid culture, is the method in which bacteria is suspended in a nutrient medium. Liquid medium allows faster bacterial growth than solid media. The process of growing *E.coli* using the liquid culture method in-vivo, involves picking a single colony from a selective plate[36]. The single colony is then inoculated into 5mL of LB medium and placed in a shaking incubator (300rpm) for 12hrs, to saturation whereby the sample solution appears turbid. The user then picks up the sample and performs serial dilution in order to obtain the desired bacterial concentration. If the bacteria are present and viable, it can then be tested for drug susceptibility, which will be discussed in more detail in the following section.

If this method could be made faster, it would be ideal in a resource limited setting to perform rapid diagnosis at under \$5. The key to making it faster is miniaturization and parallelization.

At its fundamental level bacterial culture is a simple yet robust method to identify that a particular organism is viable by visualizing it with the naked eye through amplification (colony growth). However, there are other methods that one could use to determine bacterial presence and viability. Any organism that is alive will consume nutrients and excrete waste. Thus by measuring the material that is consumed or excreted, one could have an early indicator of the viability of the bacteria even before it has divided and grown sufficiently to be visually noticed.

### **2.3.3.1 Chromogenic Media**

Chromogenic media is used in culture for the simple method for the detection of a specific microorganism. Chromogenic media contains molecules, known as chromogens. Chromogens are composed of two parts: a substrate and a chromophore. The substrate of the chromogen targets a specific enzyme produced by the bacteria. The chromogen remains colorless until an enzyme cleaves onto the substrate causing the chromophore to be released. This causes the coloration of certain bacterial colonies of interest. An example of differential media is the urease test (also known as Campylobacter-like organism test), which is used to detect the presence of *Helicobacter pylori* [37]. The test

is composed of two parts urea (nutrient), and a pH indicator phenol red [37]. Urease enzyme, which is produced by *H.pylori*, is able to hydrolyze urea to ammonia and carbon dioxide, which forms an alkaline end product, ammonia. This causes the pH indicator phenol red to turn from yellow into red, indicating the presence of the bacteria[37]. This color-based differentiation method is able to clearly and easily distinguish the presence/absence of the target bacteria. Another example of chromogenic media is the Colilert test. Colilert relies on a patented Defined Substrate Technology (DST) to detect the presence of coliforms and *E.coli*. Two carbon sources that act as nutrient indicators of Colilert are ONPG and MUG, which can be metabolized by  $\beta$ -galactosidase (coliform enzyme) and  $\beta$ -glucuronidase (*E.coli* enzyme) [38]. If *E.coli* is in fact present in the sample, its enzyme metabolizes MUG, in which the solution will create fluorescence that can be excited by UV. Additionally, if coliforms are present, the solution will change from colorless to yellow (visible by the naked eye) once the coliform enzyme breaks down ONPG [38].

#### **2.3.4 Drug Susceptibility**

Susceptibility testing is used to determine which antibiotic prevents the growth of the bacteria of interest. The result of this in vivo test determines which antibiotic will be most successful in treating the bacterial infection. Clinicians are then able to choose the appropriate antibiotic to treat the bacterial infection.

There are many drug susceptibility methods including Stokes method, Etest, Agar, and broth dilution. One of the most commonly used drug susceptibility test used is known as the Kirby-Bauer method, shown in figure 10 [39]. In this method, thin wafers containing antibiotic are placed on the agar plate, in which bacteria grow. The size of the zone of inhibition is indicative of the sensitivity of the bacteria to the drug. If the bacteria's zone of inhibition is equal to or larger than the standard zone, then the bacteria are sensitive to the drug. However, if the zone of inhibition is non-existent or smaller than the standard zone, then the bacteria is resistant to the drug[39].



**Figure 10:**Antibiotic sensitivity test with thin wafers. Produced from[40].

Another popular drug susceptibility test used is, broth microdilution, shown in figure 11 [41]. Several microtiter plates are filled with a solution of bacteria, broth and varying concentrations of antibiotic in each well. The plate is then incubated for a period of 20 hours, and then checked for bacterial growth. The wells that are cloudy are indicative of bacterial growth; whereas the wells that are clear demonstrate drug sensitivity. Results of the AST (antibiotic sensitivity tests) are reported as the minimum inhibitory concentration (MIC), which is the lowest concentration of antibiotic that prevents the growth of the microbe[41]. The size of the zone in the Kirby-Bauer method is equivalent to the MIC. Thus, a sensitivity analysis helps to determine the most effective antibiotic to inhibit the growth of bacteria and the minimum amount of drug required to prevent bacterial growth (MIC).

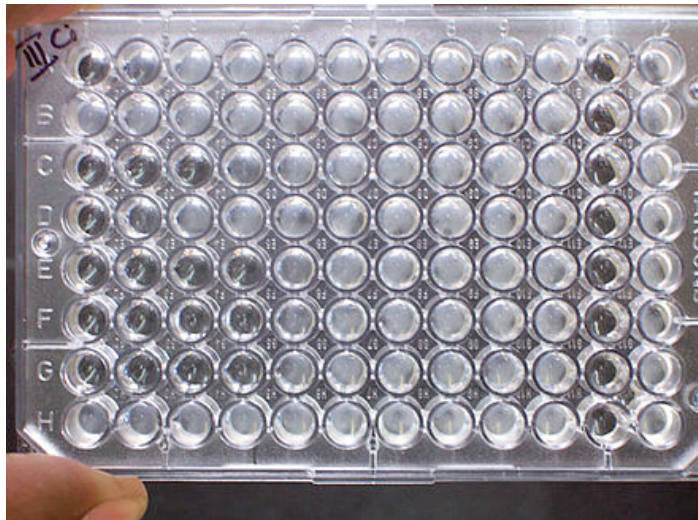


**Figure 11:** Broth microdilution test. Reproduced from [42]

## **2.4 Molecular Based Detection**

As discussed above, molecular diagnostics are a collection of techniques used to identify infectious diseases by detecting specific sequences in DNA or RNA[43].

### **2.4.1 Immunoassays**

Enzyme linked immunosorbent assay are the most common immunoassays to detect whether a certain antibody or antigen is present in a sample[44]. It is a biochemical technique that is used in immunology, for infectious disease testing[44]. Immunoassays are used to detect the presence and measure the concentration of a specific antibody that has been produced in response to pathogen exposure[44]. This is demonstrated through color change, which is quantified by the use of a spectrophotometer reading at the appropriate wavelength for the color produced.

There are three main methods, which form the basis of all ELISA's: direct ELISA, indirect ELISA, and sandwich ELISA (figure 12). The combination of these three main systems can be used to form the basis of competition ELISAs. The basic principal of ELISA uses an enzyme to detect the binding of an antigen to an antibody[44]. The enzyme converts a colorless substrate (chromogen) to a colored product; this indicates the presence of an antigen-antibody binding[44]. The most commonly used enzyme labels are horseradish peroxidase (HRP) and alkaline phosphatase (AP)[45].

Direct ELISA detection begins with the adsorption of an antigen to the sample wells in a microtiter plate[46]. Bovine serum albumin (a protein) is then added to block all other possible binding sites. The first antibody is then introduced, by which it binds to any recognized antigen epitopes[46]. This process can also be reversed so that an antibody is coated to the plate instead and a labeled antigen is introduced. When the analyte is immobilized on the microtiter plate, an enzyme-conjugated enzyme is washed over the plate, whereby the antibody binds to the immobilized analyte. Any unbound analyte and antibody is rinsed away. Next, a chromogenic substrate is introduced to the solution, such as human chorionic gonadotropin (HCG), which can be detected by ELISA. Whereas, indirect ELISA is a two-step process which involves two binding process of a primary antibody and a labelled secondary antibody[46]. An antigen is coated to a multitier plate. Next, an unlabelled primary antibody (specific to the antigen) is applied. An extra step to the direct ELISA technique is the addition of an enzyme-labelled secondary antibody that binds to the first antibody. More than one labeled antibody is bound per antigen molecule, giving it a high sensitivity[46]. Lastly, Sandwich ELISA captures and detects antigens between two layers of antibodies[45]. Since two antibodies bind to an antigen in a ‘sandwich’, it must have at least two antigenic epitope capable of binding to two antibodies. There are two antibodies that can be used for the sandwich ELISA system, either monoclonal or polyclonal, in order to capture and detect the antibody. Monoclonal antibodies have a monovalent affinity, in that they bind to the

same epitope. In contrast, polyclonal antibodies are immunoglobulin molecules with higher affinity, which can recognize multiple epitopes on any one antigen. This method exceeds sensitivity beyond that of direct and indirect ELISA because the sample does not have to be purified before analysis unlike the other two ELISA methods[45]. The most complex of the ELISA techniques is competitive ELISA[46]. This process begins by incubating an unlabeled antibody with the antigen. These antibody-antigen complexes are then added to an antigen-coated microtiter plate. Next, the plate is washed to remove any unbound antibodies. A secondary antibody that is coupled to an enzyme has specificity for the primary antibody. This is followed by a substrate to elicit a fluorogenic signal. This differs from the other ELISA techniques in that the absence of color indicates the presence of the antigen of interest in the sample.

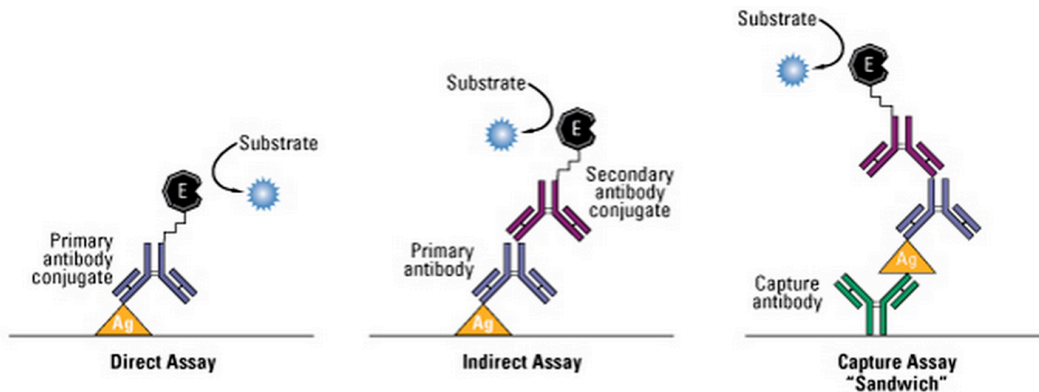


**Figure 12.** Common ELISA formats. In the assay, the antigen of interest is immobilized by direct adsorption to the assay plate or by first attaching a capture antibody to the plate surface. Detection of the antigen can then be performed using an enzyme-conjugated primary antibody (direct detection) or a matched set of unlabeled primary and conjugated secondary antibodies (indirect detection). Reproduced from [47].



While ELISA has several advantages associated with it, which includes having high sensitivity and specificity, it also has some disadvantages. ELISA is suitable for quantifying a specific protein, which is in a mix of various proteins, thus it is said to have a high specificity. However, commercial ELISA is not able to distinguish between live/dead cells, nor is it able to determine the drug susceptibility of the bacteria [48]. This technique is also costly and requires skilled laboratory technicians and specialized laboratory equipment to perform these tests. Moreover, immunoassays cannot distinguish between latent and active bacteria [49]. Considering that a wide population has latent infection but not at risk of transmission, the test is not considered the gold standard.

#### **2.4.2 Nucleic acid based technologies**

One of the most commonly used nucleic acid based methods is polymerase chain reaction (PCR) in which millions of copies of a specific piece of DNA are made[50]. Nucleic acid amplification systems, such as Polymerase Chain Reaction (PCR), shows great promise for the rapid detection of infectious disease, because of its low detection limit of 1 to ten bacilli[27]. The nucleic acid of an organism contains certain sequences that are unique to that organism. Identification of the presence of these sequences can be used as an indicator of the presence of a specific bacteria [50]. These unique sequences were identified from either the DNA or ribosomal RNA of the organism, which are conserved.

In order to liberate microbial DNA, various methods of cell lysis can be performed. There are many variations of the PCR method, such as standard PCR, real-time PCR, nested PCR, and multiplex PCR, to name a few. However the most common technique amongst the PCR techniques is real-time PCR. There are three basic steps involved in performing PCR. First, PCR undergoes a denaturation step at 95°C (figure 13) [50]. This is performed in order to separate the double stranded DNA molecule into two separate single stranded DNA's. Next, this process undergoes an annealing step at 55-60°C (figure 13) [50]. When temperature is lowered, primers attach to complimentary sequence on the original DNA strand to prevent the denatured DNA from reforming a double helix. The final step is the extension phase, which involves DNA polymerase binding to the primer and building a complimentary strand to the original template[50]. Once the replication process is complete, the process is repeated for 20 cycles to obtain one million copies, which amplifies the signal (figure 13).

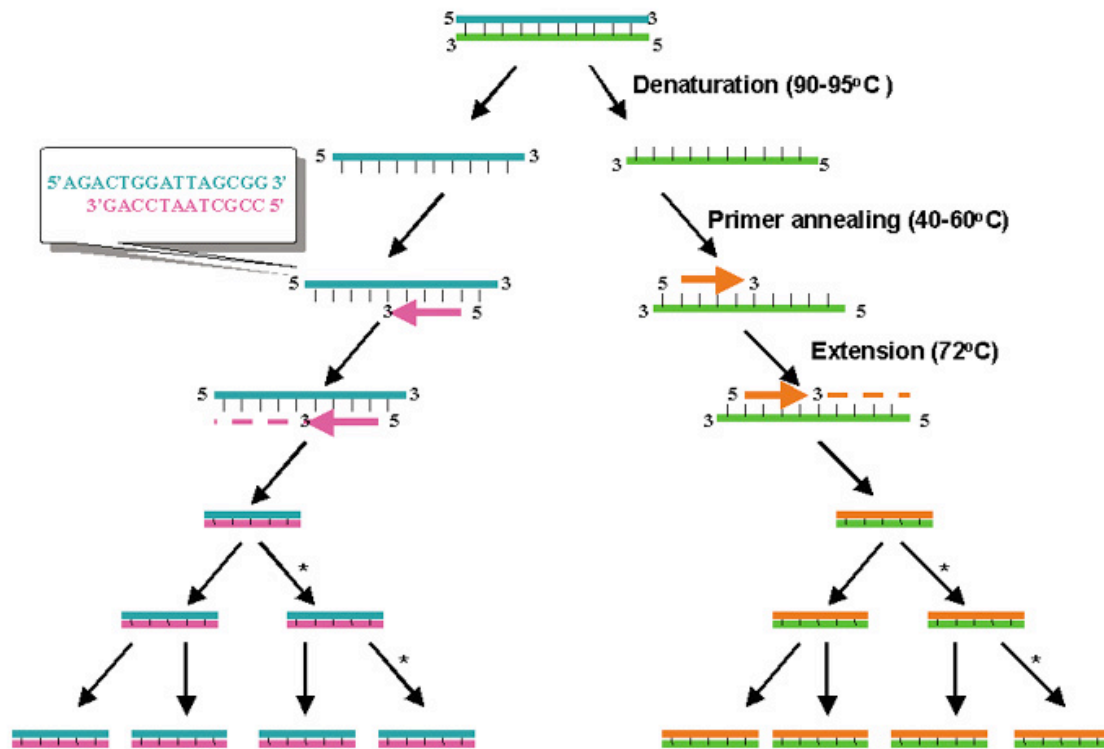


**Figure 13.** Schematic of PCR. Each cycle of the PCR includes heat denaturation of the double stranded DNA template into single strands, annealing of an oligonucleotide primer complementary to sequence being amplified, and extension of the annealed primer using a thermostable DNA polymerase and nucleotide triphosphates. Repeated cycles result in exponential, sequence specific amplification of the original target. Reproduced from[51].

PCR is particularly useful in the early detection of disease, in comparison to techniques that rely on antigen (often produced weeks or months after infection), whereas PCR produces results in a matter of minutes. Therefore, nucleic acid based testing has accelerated the process of identification of bacteria [52]. They have also made possible the identification of species that are not culture-able. PCR can also calculate the viral load

of the body, which determines the amount of virus circulating around the body[52]. Thus, PCR can count the number of bacterial cells as they undergo treatment, which can be used to detect their resistance to antibiotics. PCR is the most sensitive of the existing rapid methods to detect pathogens for infectious disease.

However, PCR techniques have many potential pitfalls due to the susceptibility of PCR to inhibitors, contamination and experimental conditions. The greatest advantage of PCR – its ability to detect very small numbers of bacteria – also proved to be its drawback. Contamination during sample preparation and through reusable equipment led to a large number of false positives[52]. Furthermore, sequence data is needed prior to experiments, to design primers for PCR. Therefore, PCR can only identify the presence or absence of a microbial pathogen. Although, this technique shows excellent promise for clinical settings it is still very expensive[52]. The reason for the high cost is due to expensive reagents (which include primers, polymerase enzyme as well as other chemicals that are needed). Moreover, complex instrumentation is needed to perform unit operations such as lysis[52], DNA extraction and amplification as well as the need to prevent non-specific contamination. In addition, it does not provide information on the viability of the bacteria and its drug resistance to multiple drugs that are available to treat it.

**Table 1.** Summary of advantages and limitations of each rapid detection [1]

<b>Detection Method</b>	<b>Advantages</b>	<b>Disadvantages</b>	<b>Detection Limit</b>
<b>Nucleic Acid-based detection (Simple PCR)</b>	<ul style="list-style-type: none"> <li>-High sensitivity</li> <li>-High specificity</li> <li>-Automated</li> <li>-Reliable Results</li> </ul>	<ul style="list-style-type: none"> <li>-Affected by PCR inhibitors, Requires DNA purification</li> <li>-Difficult to distinguish between viable and non-viable cells</li> <li>-High Cost</li> </ul>	$10^3$ - $10^4$ CFU/mL
<b>Immunological based detection (ELISA)</b>	<ul style="list-style-type: none"> <li>-Specific</li> <li>-Can be automated so that it is more time efficient and labor-saving</li> <li>-Allows the detection of bacterial toxins</li> <li>-Handles large numbers of samples</li> </ul>	<ul style="list-style-type: none"> <li>-Low sensitivity</li> <li>-False negative results</li> <li>-May result in cross-reactivity with closely related antigens</li> <li>-Pre-enrichment is required in order to produce the cell surface antigens</li> <li>-Requires trained personnel</li> <li>Requires labeling of antibodies or antigens</li> </ul>	$1 \times 10^4$ – $2.8 \times 10^6$ CFU/mL
<b>Staining (Ziehl-Neelsen)</b>	<ul style="list-style-type: none"> <li>-Prevents cells from washing away, preserves cells, kills microbes, distinguish cells</li> <li>-Cheap</li> <li>-Effective</li> <li>-Quick</li> </ul>	<ul style="list-style-type: none"> <li>-Inability to determine motility, distortion of cell size/shape</li> </ul>	$10^3$ - $10^4$ CFUL/mL

<b>Culture (Solid Agar Plate)</b>	-Simple -Inexpensive	-Slow turnaround times	10-100 CFU/mL
-----------------------------------	-------------------------	------------------------	------------------

## 2.6 Summary

In this chapter, the background of the thesis is introduced. A rapid and accurate method to detect the presence, viability and drug susceptibility of the bacteria in clinical and food samples is critically needed. As previously mentioned, primary laboratory diagnostic techniques such as the gold-standard culture-based technique and smear microscopy are limited to patients with advanced infection, and have a long turnaround time for diagnostic results. Although molecular diagnostics (i.e. nucleic acid based diagnostics or immunoassays) provide sensitive and specific diagnosis, they require highly skilled personnel to operate, sophisticated instruments, and have high costs associate with them, deeming them an impractical option in resource-poor settings. To solve this problem, a low-cost microfluidic device capable of rapid detection of bacterial infections is needed. Based on review and analysis, combining miniaturization with liquid culture and integrating a fluorophore for the detection of metabolic changes within the volume are advantageous to be applied on developing the novel device.

## **Chapter 3.**

# **Device Design, Working Principle, and Fabrication**

As described in the previous chapter, the current diagnostic process is multi-layered, accumulative, resource intensive and takes long time. Bacterial culture is the gold standard but has long turnaround times. Alternate methods such as staining, immunoassays and nucleic acid assays are faster but are either not definitive or expensive and don't provide all the information sought by the medical professional in formulating a treatment and saving lives. Thus, often times several tests get ordered, in the face of inconclusive evidence. The device presented in this thesis should be able to detect the presence, viability, and drug susceptibility of bacteria like the culture test but with significantly shorter turnaround times. This chapter introduces the fabrication techniques and materials used in the assembly of the device. The process of sample preparation is also covered in this chapter. Then the surface modification and experimental loading that is done to make the inside of the wells hydrophilic and the outside hydrophobic to dispense the liquid is discussed. Next, the process flow for PDMS device fabrication

using photolithography technique is detailed. Lastly, the image processing technique that is used to measure fluorescent intensity is discussed.

### **3.1 Device Design and Working Principle**

Dating back to 100 years ago, culture mediums used to be inoculated in larger volumes (10 mL or more) in order to test for a particular characteristic of a bacterium. In addition, these volumes were inoculated in individual test tubes, which proved to be a tedious task. As time progressed, researchers have developed the culture test so that several cultures can be grown serially in order to study large number of isolates This was accomplished in order to inoculate multiple cultures at once. In 1975, Fung and Hartman introduced culture volumes that were miniaturized to reduce the volumes of reagents from 10 ml to 0.2 ml volumes in microtiter plates so that multiple cultures were processed simultaneously [53]. These were performed in 96 well plates with a multipoint inoculator, which saved time and effort. Each transfer in the conventional culture test would represent 96 separate inoculations. Miniaturized systems have proved to be accurate, efficient, labor saving, space saving and cheaper than the conventional procedure.[54]



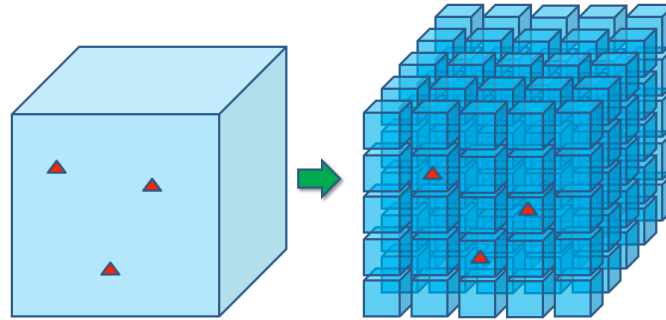


**Figure 14:** Miniaturization and compartmentalization of a milliliter volume into several microliter volumes. The concentration of bacteria (red triangles) is small in the large volume. However, the concentration is high in some of the micro-volumes while it is zero in others.

Thus, by miniaturizing the volume even further to microliter and nanoliter volumes to detect specific metabolites of bacteria turnaround times can be reduced significantly. Consider the case in figure 14, when the 1 ml volume is split into million individual 1 nL volumes. Some of these volumes have bacteria in them and the others don't. Each nanoliter volume now contains a specific concentration of dissolved molecular oxygen. Oxygen content will be consumed in volumes that have bacteria whereas volumes that contain no bacteria will remain unchanged. The result is a highly sensitive diagnostic tool to rapidly detect the production/consumption of metabolites. If one is able to segment a volume of fluid into micro or nanovolumes and analyze for presence or absence of metabolites in parallel across those millions of micro/nanovolumes then the process of detection for viability of bacteria can be

accelerated. This simple example demonstrates the power of miniaturization and parallelization, which is the main principle behind the proposed device that will be discussed in further detail in the following chapter.

### **3.1.1 Design Criteria**

The minimum amount of blood withdrawal from patients for accurate culture tests is 0.5mL [55]. Thus, a device requirement is that the nanowell array must be able to hold a minimum of 0.5mL of volume. It should also be designed such that it has quick and easy sample preparation and bacterial solution loading, with fast turnaround times. That way, medical practitioners wouldn't need trained personnel to perform these tests.

Several key design criteria include:

- 1) Developing a device that can be used to provide information on the presence, viability and susceptibility of bacteria.
- 2) Achieving fast turnaround times, where the measurement time is under an hour.
- 3) Simple and easy sample preparation and loading process
- 4) Maximizing the portability of the device.

Based on the design criteria listed above and the methods for a diagnostic device, this thesis discusses in further detail a device to meet those requirements.

### 3.1.2 Device Design

This thesis presents a microfluidic device that is 1-2cm<sup>2</sup> in size for most experiments, as a proof of concept before designing a larger array of nanowells to hold the target volume of 0.5mL of solution. This device is designed to be composed of an array of nanowells with diameters (100-1000 $\mu$ m), depth of 100  $\mu$ m, and volume that varied from (1nL-100nL). The well depth was kept at 100  $\mu$ m to minimize vertical diffusion of bacteria and so that the bacterial solution could deposit with ease.

Various sized arrays of nanowell devices were fabricated in the range of 1nL to 100nL and diameters between 100 to 1000 $\mu$ m, with dimensions of: 100  $\mu$ m (1 nL), 225  $\mu$ m (5 nL), 265  $\mu$ m (7 nL), 340  $\mu$ m (11.5nL), 360  $\mu$ m (13 nL), 500  $\mu$ m (25nL), and 1000  $\mu$ m (100nL). A range of volumes ranging from 1nL to 100nL was chosen in order to study the affect of size on the turnaround times of results. The size of nanowells tested remained at a size no smaller than 1nL in order to trap the bacterial solution with ease and to simplify the fabrication process.

The spacing between nanowells was chosen to be equal to the diameter of the nanowells, so that there was minimal oxygen diffusion in PDMS walls between the nanowells.

Lastly, different shaped wells (circular vs. square) were tested in order to study the effect of geometry on the capability of the wells to fill, and it was noted that geometry had no effect.

### **3.2 Working Principle**

Here, metabolic monitoring of the growth of bacteria is applied in nanoliter well arrays to increase the speed of detection of bacteria, its viability and its drug resistance. It is demonstrated in this thesis that the smaller the nanowells, the faster the detection time. It is also demonstrated that minimal sample preparation method is required for this method making it suitable for resource poor settings. This method could be a viable alternative to the current culture method and could be easily implemented in a wide variety of settings.

A method is devised to detect the bacteria at fast rates by measuring oxygen consumption (metabolic marker). The device consists of an array of nanoliter wells. The inside surface of the wells are made hydrophilic while the top surface is made hydrophobic (figure 15; part 1). When a sample is dispensed and spread on the device, the sample will easily penetrate the wells and dispense into it while avoiding the surface.

An optical, oxygen quenching fluorophore  $\text{Ru}(\text{BPY})_3$  as well as growth media[56] that facilitates growth of specific bacteria is mixed with a sample and dispensed onto the surface of the device containing an array of nanowells (figure 15; part 2). Since bacteria

are aerobic, they consume oxygen that is present in the medium during metabolism and depletes the oxygen in the surrounding environment, producing fluorescence. The separation distance between the nanowells is determined by the permeability of the material to oxygen over the duration of the detection. Drug resistance can also be probed by adding the appropriate drug to the broth and measuring growth or lack of it through fluorescence. A glass slide is then swiped across the surface (like a squeegee), which allows the bacterial solution to deposit and compartmentalize into the specific wells (figure 15; part 3).

Once compartmentalization of liquids within the defined wells is completed, a glass slide seals the nanowells as to prevent evaporation of the sample (figure 15; part 4, 5). In which time, the bacterial solution is then sealed within the well and is immediately taken to a microscope to image the fluorescent intensity (metabolic measure of oxygen) changes during that process (figure 15; part 6). The segmentation of the sample into thousands of individual nanoliter wells digitizes the sample and has some benefits. Consider a typical sample that is several hundred nanoliters in volume contain a certain concentration of bacteria. At high concentrations, the concentration of bacteria in each well is the same as the overall concentration of the sample. However, at low concentrations, if the sample were segmented into thousands of smaller volumes then some of the wells will contain the bacteria of interest while others will not. The process of digitization of the samples creates some wells where the local concentration of bacteria is

several times higher than the overall concentration in the sample and others where there would be no bacteria. Therefore, by digitizing the sample and measuring the metabolic markers in each of the wells simultaneously, one could arrive at detection of the bacteria much faster than in a larger homogeneous sample. This is the working principle behind fast metabolic monitoring of bacteria.

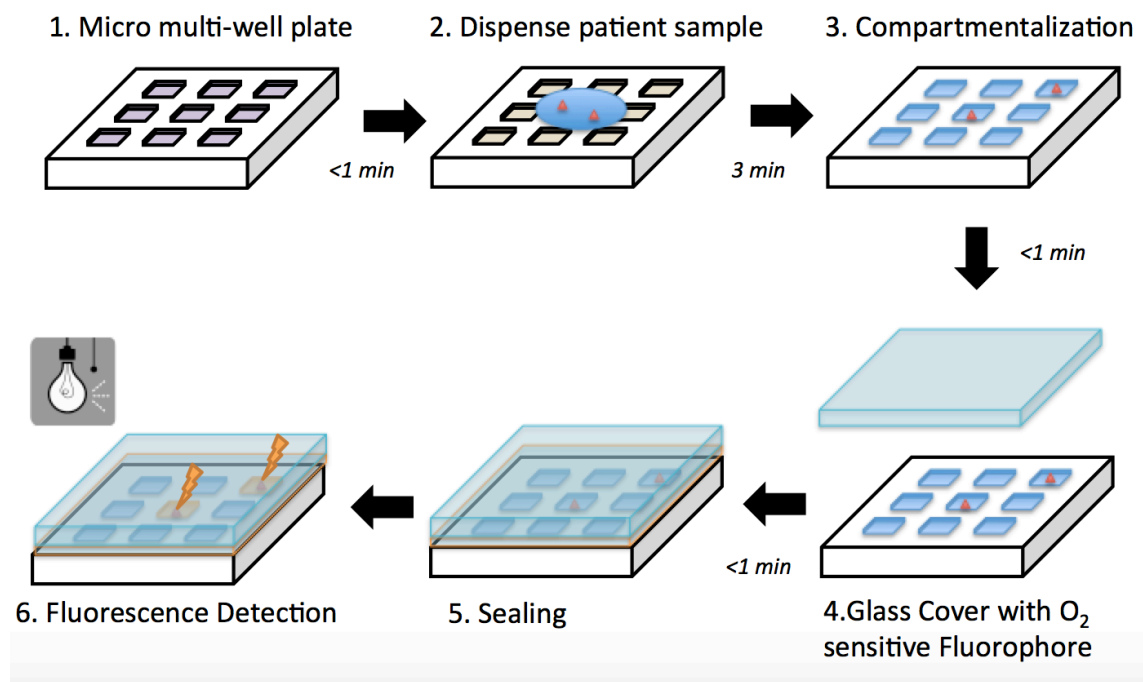


**Figure 15:** Loading of solution and sealing for imaging procedure.

### **3.3 Materials and Methods**

#### **3.3.1 Materials**

##### **3.3.1.1 Silicon wafer**

Silicon wafers are used as a substrate in the photolithography procedure, in order to make a mold master for molding polymers. Silicon wafers (mechanical grade, 3", 500  $\mu\text{m}$  thick) were purchased from University Wafer Co., USA. A silicon wafer was chosen for this experiment because it provides a good adhesion to SU-8 [57].

##### **3.3.1.2 SU-8 Photoresist**

The mold is made with the epoxy resin SU-8 with negative photoresist, using photolithography. The process flow for the device fabrication is shown in figure 16. Negative photoresist Su8-100 and developer were acquired from Microchem Co., USA. SU-8 100 can produce a film thickness ranging from 1-200 $\mu\text{m}$ . Upon exposure to light, the photoresist polymerizes and is mechanically stable.

SU-8 100 photoresist is spun on a Silicon wafer at 1,700 rpm to produce a layer of 100- $\mu\text{m}$  thicknesses. This layer was patterned using photolithography and produced square or circular shapes of sizes that varied from 100-1000  $\mu\text{m}$  features. That constituted the mold to form the array of nanowells.

### **3.3.1.3 Polydimethylsiloxane (PDMS)**

Next, polydimethylsiloxane (PDMS) prepolymer (base: curing agent = 10:1) was cast on the mold, cured and peeled off to replicate the pattern of the mold forming an array of nanoliter wells. Polydimethylsiloxane is the most commonly used silicon in academic studies of microfluidics[58]. There are many advantages to using PDMS over other materials, which include: ease of replication of submicron features, optical properties (transparent in the range 190-700nm wavelength), non-toxic, low-cost material, and permeability of oxygen[59].



**9 steps of lithography process**

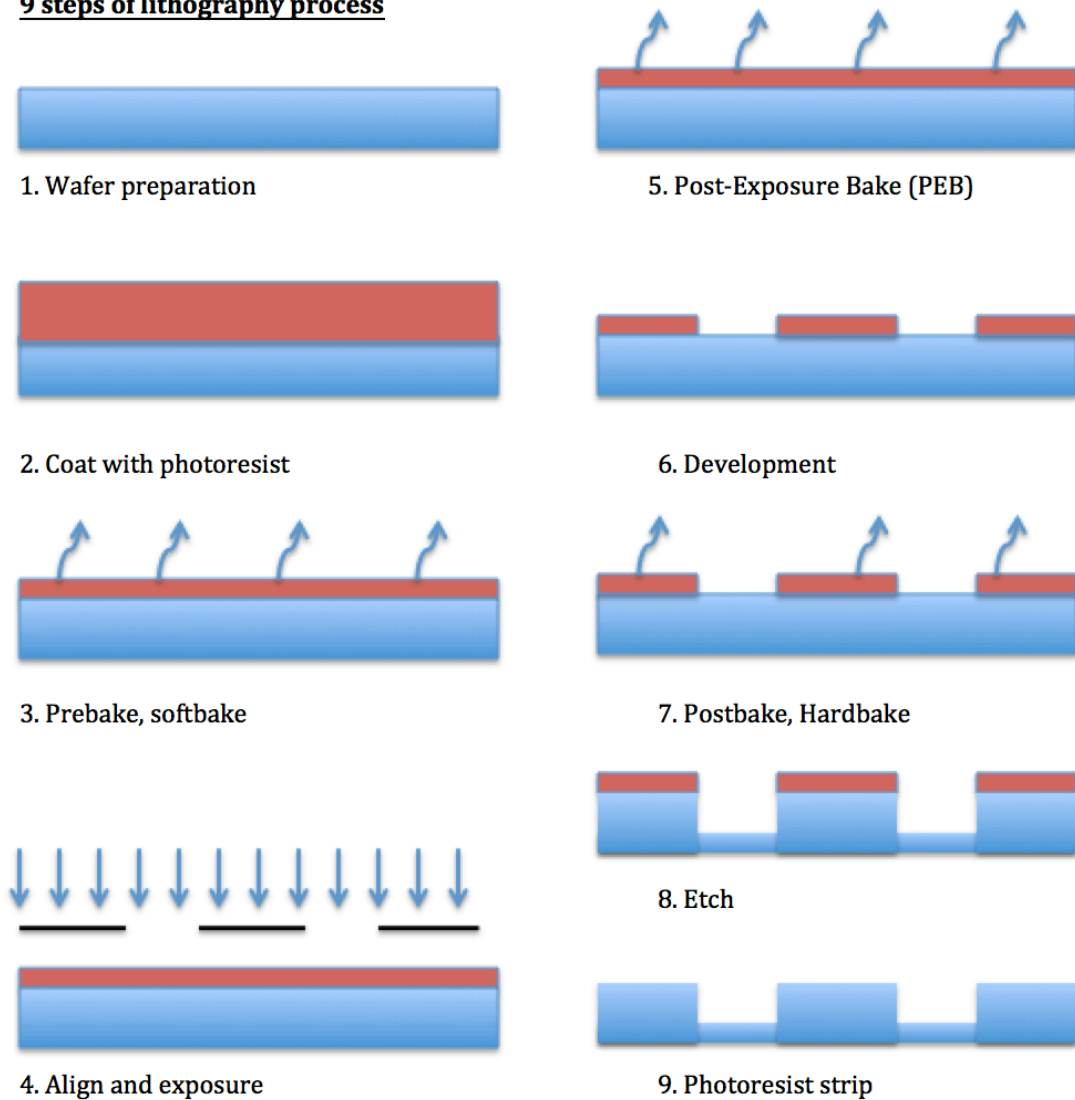


**Figure 16:** The flow process of the device fabrication. 1) silicon wafer is cleaned and prepared for use 2) 100um thickness of SU8 is deposited on the surface of the silicon wafer 3) It is then soft-baked so that the su8 layer is densified 4) alignment and exposure for patterning of the first SU8 layer. 5) Post-exposure bake is done to reduce the standing wave effect 6) Next, Development is used to control development uniformity and Etch. 7) Postbake, hardbake used to stabilize and harden the photoresist.8) Next, these patterns are transferred into the substrate through etching. 9) Lastly, after the wafer has been etched, the remaining photoresist must be removed.

### 3.3.2 Fabrication Steps and Methods

The device fabrication includes the following 2 steps:

#### 1) Master mold fabrication

In the conceptual design the nanowell device consists of features of 100 $\mu\text{m}$ . The silicon moulds of the nanowell array for the casting of PDMS are fabricated using the photolithography process, as shown in figure 16, part 1. The photoresist used for this particular experiment is SU-8 100, with viscosity of 51500 cSt. To achieve a thickness of 100  $\mu\text{m}$ , a spin speed of 3000rpm should be achieved, as shown in figure 16 part2. Pre-bake for 10 min at 65C and softbake at 95C for 30 min. (figure 16 part 3). Then align the mask with the wafer and attach them when alignment is done (figure 16 part 4). Next, expose the wafer to UV light through the mask for total exposure energy of 160mJ/cm<sup>2</sup> (figure 16, part 5). Afterwards, place the device in a developer for 10min to achieve the desired thickness, as shown in figure 16 part 6. Next, hard bake the wafer on hot plate at 150°C for 30min (figure 16 part 7). The device well then be etched and the photoresist will be stripped as shown in figure 16 part 8 and 9. Photomasks with desired nanowell patterns and dimensions were completed with Inventor (Autodesk Inc., San Francisco, USA), which were in turn sent to *CAD/Art Services Inc.* for ultra-high-resolution printing on a transparency sheet. More information provided in appendix A.

## **2) Nanowell Casting**

As discussed, the mould is designed using a photolithography process, whereby SU-8 is used as the photoresist to create 100  $\mu\text{m}$  feature sizes as shown in figure 17(i), 17(ii) and 17(iii). Next, the PDMS nanowell array was fabricated using a soft-lithography method. The PDMS base and cross-linker were mixed in a 1:10 ratio and poured on top of the master mold (as shown in figure 17 vi). It was then left to cure in the oven, at a temperature of 60C for 4 hours. Then the polymerized PDMS was peeled off of the master mold (figure 17 v). The nanowell array is then cut-out in a square shape (figure 17iv and 17vii). More detail provided in appendix A.

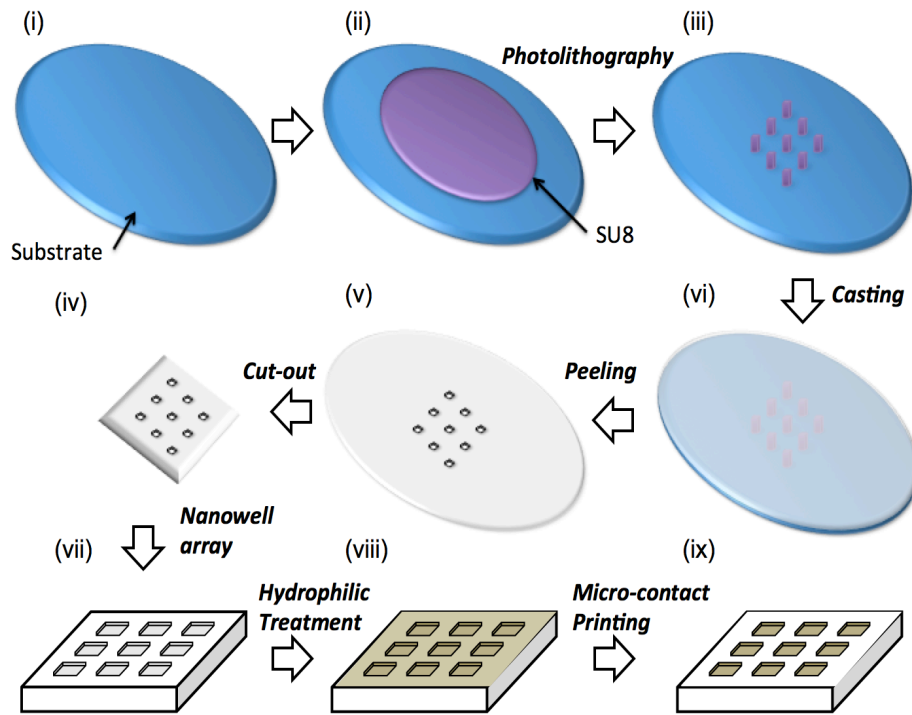


Figure 17. Fabrication process of nanowell array.

### 3) Surface Treatment

Naturally, PDMS is hydrophobic. However, it undergoes surface treatment in order to achieve hydrophilic inner wall of the nanowells and an outer hydrophobic surface. The entire top surface of the PDMS is coated with a hydrophilic treatment, known as n-Wet 410 and left overnight as demonstrated in figure 17 viii. The next day, the nanowell array is then micro-contact printed against a 1:10 ratio of PDMS and curing agent, so that the top surface becomes hydrophobic while the inner surface remains

hydrophilic as shown in figure 17 ix. The device is then placed on an oven at 60C for 30 minutes, and once dry it is ready to be used.

### **3.4 Sample preparation**

#### **3.4.1. Materials**

##### **3.4.1.1. Culture medium**

A culture medium (growth medium) is a nutritionally rich liquid or gel in which bacteria is cultivated to support its growth. The media selected for the growth of *E.coli* was Luria-Bertani which consists of a mixture of 10 g tryptone, 5 g yeast extract and 10 g NaCl.

##### **3.4.1.2. Ampicillin**

Ampicillin is an antibiotic used to treat certain infections caused by bacteria. An ampicillin concentration of 100 mg/mL was prepared and used in this study for two different purposes. In the first set of experiments, where *E.coli K12* is used, ampicillin is added because *E.coli K12* is ampicillin resistant so it has no effect on the *E.coli strain* but kills off any other strains of bacteria. In the second set of experiments, because the *E.coli strain OP50* is ampicillin sensitive, the drug is used to test drug susceptibility of the bacteria.

### 3.4.1.3. Bacteria

*E.coli* is a gram-negative bacterium due to its thin cell wall, with dimensions of: 0.5  $\mu\text{m}$  in width by 2  $\mu\text{m}$  in length. It is an inhabitant of the lower gastrointestinal tract of animals. *E.coli* is able to survive many variable conditions, which makes it an ideal bacterium to work with. Knowledge gained from experiments on *E.coli* is expected to be able to be applied to other bacterial species. Some advantages to using *E.coli* is that it is a single celled organism that is able to grow quickly as its doubling population is 20minutes, it can survive in many abnormal growth conditions, and is non-pathogenic.

In this thesis, all experiments were done with *E.coli*. This bacterium was used as a model organism to study the presence, viability and drug susceptibility of bacteria using the nanowell array designed. There were two different types of bacteria used for the experiments. The bacteria used for the majority of experiments was an ampicillin resistant *E.coli*, strain *K12*. MG1655 (Purchased from ATCC 27325) The bacteria used for drug susceptibility was *E.coli* strain *OP50* which, unlike *E.coli* strain *K12*, is ampicillin sensitive.

#### **3.4.1.4 Fluorophore**

An optical oxygen quenching fluorophore, Ru(BPY)<sub>3</sub>, was chosen to detect changes in levels of dissolved oxygen within the nanowells. The powder of Ru(BPY)<sub>3</sub> (ruthenium tris(2,2'-bipyridyl) dichloride hexahydrate) was obtained from Sigma-Aldrich (#224758) with excitation  $\lambda = 450\text{nm}$  emission  $\lambda = 625\text{nm}$ . It is reported that Ru(BPY)<sub>3</sub> is able to reliably detect and differentiate between oxygen levels by as little as 8  $\mu\text{M}$ [60], which is especially critical for the design criteria of this project.

#### **3.4.1.5 Hydrophobic coating of glass**

Glass used to seal the nanowell array was coated with a hydrophobic layer in order to seal the solution in the nanowells with ease, so that the liquid does not adhere to the surface of the glass. The hydrophilic surface modification agent (N-Wet 410) was gifted by Enroute Interfaces Inc., and one part of the n-Wet 410 solution was diluted with 9 parts of toluene giving a final concentration of 10% w/w. Glass slides (Corning, 75x25x1mm) were used to sandwich the nanowell device. A commercial surface modification agent, Aquapel applicator was obtained from Aquapel® Glass Treatment, and was used to make glass slides hydrophobic, methylcellulose MC (M-0262) viscosity of 2% aqueous solution at 20°C, 400 centipoises (Sigma).

#### **3.4.1.6 Artificial sputum**

The sputum was prepared by mixing 2%(w/v) methylcellulose (Sigma M-0262) in 1000mL of DI water[61], which resulted in a viscosity of 0.4 Pa-s at room temperature [62]. This viscosity matched that of mucoid, which was reported by Maria Teresa Lopez-Vidriero et al[63] to be 0.42 pa-s.

#### **3.4.2 Sample preparation**

##### **3.4.2.1 Bacteria preparation**

A colony of ampicillin-resistant bacteria was picked from an agar plate and inoculated into a 4mL liquid medium, with 4ug of ampicillin. *E.coli* was then left overnight to grow (12 hours), and picked up in the morning. Once it was picked up, a spectrophotometer is used to measure the O.D.<sub>600</sub> to determine the concentration of bacteria. However, the linear absorbance range of the spectrophotometer is between 0.1 and 1. Bacterial samples were diluted considerably to obtain reasonable counts. They were diluted to a concentration of  $10^6$  cells/mL. The objective of the serial dilution in this case, is to estimate the concentration (number of bacteria) of the original sample by counting the number of colonies cultured from serial dilutions of the sample, and then back track the measured counts to the original concentration. This step was important for consistency in the results.



An O.D.<sub>600</sub> value of 1 was used for experiments, which correspond to  $1 \times 10^9$  cells per ml culture (obtained from *E.coli* standard growth curve).

Next, the sample that was left overnight undergoes serial dilution. Precise serial dilution of a sample is done such that the exact concentration can be obtained for the experiment to become a success (i.e.  $10^8$ ,  $10^7$ , etc). Without serial dilution it would be very difficult to measure the exact concentration of cells per ml.

Therefore, in order to get accurate concentrations for the experiments, the bacteria were grown to a known concentration ( $1 \times 10^9$  CFU/mL). This corresponds to growing the bacteria to an early stationary phase (O.D.<sub>600</sub>=1.00), harvesting them immediately while they are under minimal stress conditions, and inoculating them into a fresh medium with a tenfold dilution. Had the bacteria been picked up in the log phase (instead of early stationary phase), the bacteria would still be undergoing cell division (doubling time, 20min), making it difficult to know how many bacterial cells were in a given sample. Thus, it is key to harvest bacteria in the stationary phase where bacterial concentration remains constant.

It is important to note however, that a newly inoculated culture (serially diluted) restarts at the beginning of the growth curve (lag phase) once again. It does not begin growing immediately - this is known as the lag phase. Although bacteria in the lag phase do not undergo any cell growth, they have an active metabolic activity. A key advantage

to the detection system presented in this thesis is that it allows the user to monitor metabolism of the bacteria in real-time instead of waiting on the proliferation of the bacteria, which is a slower process. This means that at the lag phase, where many detection systems don't work, the technique proposed in this thesis would be able to detect and monitor metabolic changes to determine bacterial presence.

To test the device, three samples are prepared:

**1) GFP tagged bacteria**

*E.coli K12* is an ampicillin resistant strain of bacteria that is GFP tagged. A solution was prepared consisting of LB media, ampicillin, and *E.coli K12* and imaged to study the ability of bacterial growth to occur in a nanowell setting.

**2) GFP tagged bacteria with fluorophore**

A solution of *E.coli K12* (GFP tagged, ampicillin resistant bacteria), ampicillin and LB media (purchased from Sigma-Aldrich), with the addition of 0.3mg/mL ruthenium fluorophore (purchased from Sigma-Aldrich) was prepared and sealed in the nanowell array to be imaged. The oxygen quenching fluorophore, ruthenium, was added to detect the metabolic changes in bacteria, in this particular case, the oxygen uptake. This information was used to study the presence, and viability of bacteria for different concentrations of bacteria. The concentration of the fluorophore was selected in a way

that a 96 well plate was prepared and the different concentrations of ruthenium were tested. A range of fluorophore concentration were tested between 0mg/mL to 5mg/mL. However, when testing this on the bacterial sample it was evident that there was a higher rate of cell death with higher concentrations of fluorophore. Concentrations that exceeded 1mg/mL resulted in inaccurate measurements. Regardless of bacterial concentration chosen at concentrations of fluorophore that exceeded 1mg/mL, fluorescent intensity did not increase as expected. Instead, the fluorescent intensity graphs were nearly identical to control tests that were performed with only ruthenium and media (no bacteria added). Concentrations lower than 1mg/mL did not demonstrate any signs of cytotoxicity, because when bacteria were present in the sample, there were increases in fluorescent intensity. Thus, it was evident that concentrations below 1mg/mL were ideal. It was found through trial and error, with 0.1 increments starting at zero and ending at one, that the ideal concentration to use was 0.3mg/mL because it had the greatest fluorescent intensity changes as compared to other concentrations.

### **3) Bacteria with fluorophore and drug**

In order to study the drug susceptibility of bacteria, a drug sensitive strain of *E.coli* was used. OP50 is ampicillin sensitive strain of bacteria, which was used to study the ability of the fluorophore to detect changes in bacterial growth when a drug is added. A sample solution of 4 mL LB media, with a single colony of *OP50* from an agar plate is

mixed in a test-tube and left in a shaking incubator overnight (12 hours). When the bacteria is harvested the next morning, a spectrophotometer is used in order obtain an optical density (O.D.600) of 1, which indicates a concentration of  $10^9$  CFU/mL [64]. Accordingly, the bacteria can be serially diluted to a specific concentration of interest. In the first test, growth of the *OP50 strain* of *E.coli* was tested without any drug added. Another test was performed, whereby the drug was added, and the correlation between oxygen uptake of bacteria (metabolism) and drug susceptibility was drawn.

### **3.5 Sample Loading and Experimental Setup**

#### **3.5.1 Sample loading**

Once the PDMS undergoes surface modification (as described in the working principle), to make the inside of the wells hydrophilic and the top surface hydrophobic, the bacterial solution is dispensed on the surface, in which it is compartmentalized. The device is then sealed with a glass and imaged with a microscope, to study fluorescence intensity of the oxygen quenching fluorophore.

#### **3.5.2 Experimental Loading**

The experiment was setup in that once the nanowells were filled with solution; it was sealed and sandwiched between two glass slides. A confocal microscope (Axiovert 100; Zeiss, Thornwood, NY) is used in the experiments. Because a confocal microscope is imaging only a thin slice of the nanowells, it is important to be imaging the correct

spot. First, the plane in which the bacteria are located is identified and the measurement of the fluorophore dye is made at the same location.

In order to match the excitation spectrum of Ru(Bpy)<sub>3</sub>, the argon laser operating at 458 nm, with an output energy of 15.0 mW, and an optical low pass filter of 585nm was employed for the experiments described here.

### **3.5.3 Image analysis**

Once experiments were completed, offline image analysis of the fluorescent intensity within the wells was calculated by using the MBF ImageJ plugins bundle (Tony Collins, McMaster University, and Wayne Rasband, NIH, [rsb.info.nih.gov/ij](http://rsb.info.nih.gov/ij)). For future experiments, the use of an inverted LED microscope instead of a confocal is proposed because of its cost effectiveness. Fluorescent images acquired with a Zeiss Axiovert 100 microscope were RGB images, but were transferred to an 8-digit gray scale format by ImageJ, in this manner, the gray scale values ranged between 0 and 255 pixels. The brighter the pixel, the higher the gray scale value. The mean gray scale value was used as a parameter to represent the average fluorescent intensity of the nanowell.

### **3.5.4 Relative gray scale measurement**

The fluorescence rise starts at the initial value  $x_0$  and reaches a value of  $x_f$ , and has values at various time points in between of  $x_t$ . From these two values, a normalization of

these values can be calculated. Subtracting the fluorescent intensity value of each individual time point from the initial value was done to normalize the data to a value of zero, for the majority of experiments. The difference between the values: Normalized fluorescent intensity =  $x_0 - x_t$  for the majority of the datasets. However, dividing each individual value of the time point of the experiments by the initial value normalized the experimental values obtained for the OP50 strain of E coli bacteria, and normalized to a value of 1. Therefore, the normalization expression for fluorescence for that experiment is the ratio of  $x_t/x_0$ .

### **3.6 Summary**

In this thesis, the development of a device that can be used to provide information on the presence, viability and susceptibility of bacteria has been designed to achieve fast turnaround times through miniaturization. It also meets the design requirement in that it should allow for a simple and easy sample preparation and loading process. Through photolithography, small features of 100um were designed for the depth of the nanowells. With soft-lithography, the PDMS was cast onto the mould that was designed and then peeled to achieve the nanowell array. Surface treatment was then performed on the device in order to allow compartmentalization of fluid into the wells. Sample preparation, materials used and the process for image analysis are discussed.

## **Chapter 4.**

### **Results and Discussion**

In the previous chapter, device fabrication, sample preparation and experimental setup were discussed in detail. In this chapter, a complete characterization of the device is performed. The various components of the assay are: sample dispensing, bacterial growth, bacterial viability, drug susceptibility, and nanowell dimensions. These steps have been characterized using the experimental protocols and setups described in the chapter 3.

#### **4.1 Sample dispensing**

First, the dispensing of the sample into the nanovolume wells and the reliability and the repeatability of the process was characterized. Therefore, various sized nanowell arrays were fabricated in the range of 1nL to 100nL. This range was chosen to be able to section a 1mL volume (typical volume sample) into ten thousand to one million nanowells, which corresponds to the field of view that can be visualized through a microscope and optical setup. As an initial experiment, a microfluidic nanowell array with 1225 wells (35x35) was designed and fabricated. Each of the nanovolume wells had dimensions of 100umx100umx100  $\mu\text{m}$  and a volume of 1nL. A sample of DI water with 100mg/mL (0.1% w/v) methylene blue with volume of 1.5  $\mu\text{L}$  was placed on the device

and a glass slide was used to move it back and forth on the device as shown in figure 18. The sample immediately entered the wells as its was moved on the surface and automatically segmented itself into precise nanoscale volumes. The entire well was found to fill within 5 back and forth motions (swipes) of the slide. This experiment provided an initial proof of concept that the selective hydrophilization of the wells and the gentle swiping motion of the sample can potentially be used to automatically and quickly segment a large sample into thousands of smaller ones.

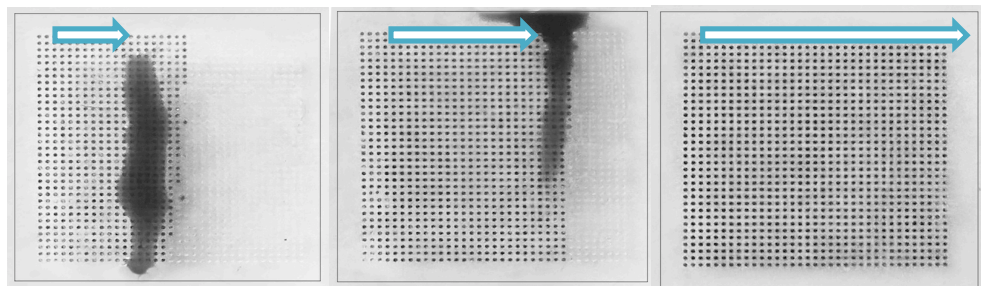


**Figure 18.** Filling a solution 1.5  $\mu\text{L}$  of methylene blue with DI water into nanowell array using a back and forth motion. Each nanowell is  $100 \times 100 \times 100 \mu\text{m}$  in dimension and holds 1nL.

Next, in order to characterize the range of sizes and volumes that were suitable for this type of sample segmentation, nanowell arrays with various sizes from 1nL ( $100 \mu\text{m}$  width and height) to 100nL ( $1000 \mu\text{m}$  width and height) were designed and fabricated. Five different sizes of square nanowells were tested. While keeping the depth at a constant value of  $100 \mu\text{m}$ , the square dimensions of the wells were changed.



Diameters varied between 100 (1nL) to 1000 $\mu\text{m}$ , (100nL) with dimensions of: 100 $\mu\text{m}$  (1 nL), 225  $\mu\text{m}$  (5 nL), 265 $\mu\text{m}$  (7 nL), 340 $\mu\text{m}$  (11.5nL), 360 $\mu\text{m}$  (13 nL), 500 $\mu\text{m}$  (25nL), and 1000 $\mu\text{m}$  (100nL). In all the experiments a solution of DI water mixed with 100mg/mL of methylene blue was used for visualization and deposited on the surface of the device. A glass slide was then brushed onto the surface to push the liquid into the nanowells. It was found that the number of swipes required per device varied with different dimensions. Each of the experiment was recorded for five different well dimensions and repeated three times per device to obtain a final graph (see figure 19). This experiment was performed to study the effect of well size on the ability for the liquid to fill the wells.

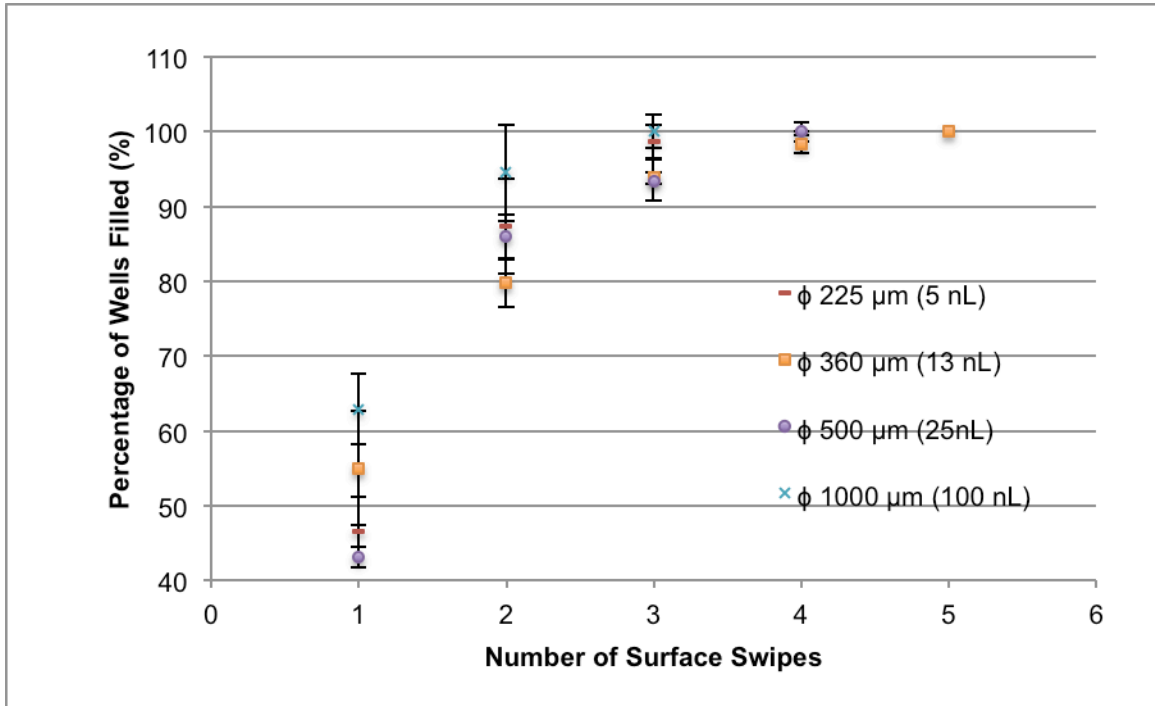


**Figure 19.** Percentage of Nanowells filled per swipe (with a coverslip) using a mixed solution of de-ionized water and methylene blue.

According to the results obtained in figure 19, the largest sized wells (100nL) filled the entire array in 3 swipes (lower surface-to-volume-ratio). Whereas the smaller sized wells 225 $\mu\text{m}$ , 500 $\mu\text{m}$  filled the entire array in 4 swipes (1 swipe more than 100nL) and 360 $\mu\text{m}$  filled within 5 swipes (2 swipes more than 100nL). This indicates that the aspect ratio has an effect on the number of swipes required when scaling down the nanowells to smaller dimensions. Surface-to-volume ratio is the amount of surface area per unit volume for an object. In the case of this device it is the inner surface of the nanowells that have undergone a hydrophilic treatment that is in direct contact with the

compartmentalized liquid. The SA/V ratio plays an important role in this experiment because the more liquid is in contact with the treated nanowells inner walls, the easier the deposition of liquid into the well. It seems as though aspect ratio had a part to play in the ability of the wells to fill quicker.

Noticing the graph, the nanowells with a lower aspect ratio, in the case of 1000 $\mu\text{m}$  well, the aspect ratio was 1:10 and thus the wells filled slightly faster. It was found that in the case of the higher aspect ratios, such as those of the 5nL volume, the aspect ratio was 1:2.25, and for 13nL an aspect ratio of 1:3.6, the nanowells took one to two swipes more in order to fill. At lower aspect ratios faster filling of wells occurs, as can be seen in the graph. This occurs because at the microscale it is easier for liquid to deposit and fill shallow nanowells. The reasoning behind this is that at lower aspect ratios the liquid to solid interface will be have a larger contact angle (i.e. 90 degrees) as opposed to higher aspect ratios which will likely have a smaller liquid-solid interface contact angle. This in turn, will likely cause bubble formation. Once an air bubble forms at the microscale it is difficult to remove [65]. Thus, high aspect ratios at the microscale are often unfavourable.

In addition, evaporation may be a limiting factor when scaling down to much smaller sizes. As reported by Taylor and Walt, filling the nanowells becomes a difficulty at much smaller scales, evaporation becomes much more significant at 25 fL [66]. Evaporation of the solution was studied once nanowells were filled, and found that

shallower wells evaporated faster than the deeper wells. Therefore an optimum of the well width to height is desired and 1:1 is suitable.

#### **4.1.1 Effects of viscosity**

The ability of the solution to compartmentalize within the nanowell array was studied using liquids of different viscosities ranging from water (0.001 Pa-s) to high viscosity shear thinning liquids such as xanthan gum (59.96% water/40% glycerol/0.04% xanthan gum)[67], protein rich solutions such as milk (viscosity of 0.003 Pa-s) and artificial sputum (0.4 Pa-s)[61] were used to study the effect viscosity has on the ease with which the wells compartmentalize the liquid. These tests were conducted because in real-life applications the user would insert blood samples or sputum samples into the device to determine whether the patient is sick or not. Thus, to understand the properties of these fluids and their behavior on compartmentalization are essential to developing our device. Thus, three repeats of each experiment were recorded and averaged out, as shown in figure 20.

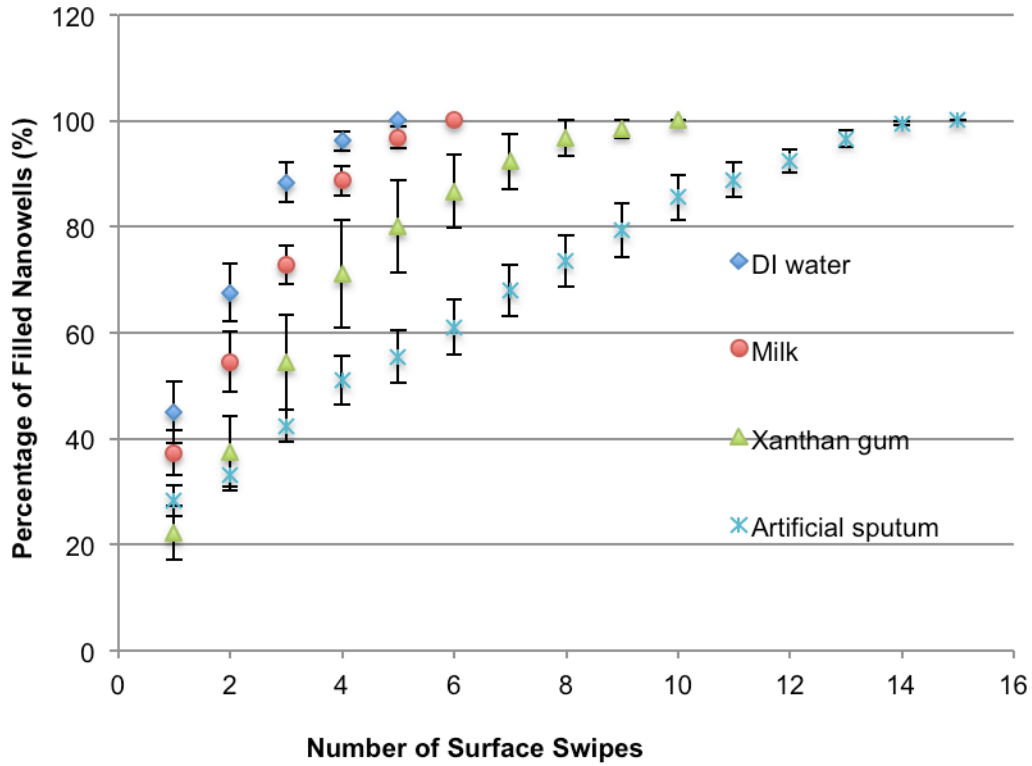


**Figure 20.** Percentage of wells filled with each swipe, of a 1nL array, with solutions of different viscosities: DI water (0.001pa-s), milk (0.003pa-s), xanthan gum (non-Newtonian fluid), and artificial sputum (0.4pa-s).

Based on experimental results (Figure 20) all the fluids were able to fill the wells. However, there was an evident trend that seemed to demonstrate that fluids with lower viscosities (DI water) required a fewer number of swipes to fill the wells as compared to fluids with higher viscosities (i.e. artificial sputum). Studying the number of swipes taken to achieve a full-compartmentalized array for DI water took on average 5 swipes, in comparison to artificial sputum (nearly 400 times higher viscosity to water) that required

a total of 15 swipes to fill the entire array of nanowells. That means in order to achieve a full array of nanowells at the highest viscosity, which was tested for, 0.4 Pa-s, it is evident from the graph that it required an additional 10 swipes in comparison to DI water (0.001 Pa-s). Further, another test was conducted in which milk (0.003 Pa-s) with a viscosity similar to that of water, was used to fill the nanowells, to determine whether a protein-rich solution would affect the compartmentalization of the liquid, however, it only required an additional swipe to DI water. This was expected, given they had the similar viscosities. A viscoelastic, shear thinning, blood analogue polymer solution, xanthan gum (0.3% xanthan solution mixed with water), was used to model pediatric blood, with viscosity 0.087 Pa-s [68]. Xanthan gum, a non-Newtonian fluid was tested for its ability to compartmentalize with ease, and according to figure 20, it seemed to require 10 swipes in total (5 additional swipes in comparison to water) to completely fill a nanowell array. Since water and milk have very similar viscosities, they are fluid and easily are able to compartmentalize into the nanowell array. While xanthan gum has a higher viscosity it can be seen that it required more 5 more swipes than water. The highest viscosity fluid, known as artificial sputum, requires the most number of swipes to fill the nanowell array. This phenomenon can be explained with capillary action. Capillary action in this case occurs when the fluid droplets are pulled into the nanowells. There is a strong adhesion within the liquid molecules themselves, however the cohesive forces between the liquid molecules and the walls of the nanowells (hydrophilic treated) are stronger. Thus,

because cohesive forces are stronger than the adhesive forces, capillary forces allow the liquid to move into the nanowells. The fluid is confined into the nanowells by making the top surface of the nanowell hydrophobic[69]. For hydrophilic surfaces, the solid surface free energy is high, making it easier for the liquid to fill in the wells as compared to hydrophobic materials that have low surface free energy..

Viscous forces on the other hand, dampen the movement of the liquid into the well. The relationship between viscosity and capillary forces can be described using the capillary number. At the microscopic level, the movement of fluids into small spaces (i.e. a nanowell), is dependent on the capillary forces and viscous forces, as shown in equation 2. Where  $v$  is the fluid velocity,  $\mu$  is the viscosity and  $\sigma$  is the surface tension. Capillary forces (no units) dominate when the  $N_c$  is approximately  $10^{-2}$  [70]. The equation for determining the capillary number is shown below:

$$N_c = \frac{v\mu}{\sigma} \tag{1}$$

Calculations of the capillary number were performed in order to study the relation between surface tension and capillary forces. It was found that milk had the smallest capillary number of  $6.4 \times 10^{-5}$  while water had a capillary number of  $1.4 \times 10^{-5}$ . It is reasonable that the capillary number of milk was lower than that of water, because the surface tension of milk happens to be less than that of water due to the presence of free

fatty acids and proteins appear to be surface active-constituents. A low capillary number is indicative that the capillary effects are stronger than the viscous effects. This means that the nanowell array will fill completely with fewer swipes. The graph however, shows that milk requires one swipe more than DI water in order to attain a completely filled array. Next, xanthan gum (0.3%) and artificial sputum were calculated in order to study the capillary number, which returned a value of  $5 \times 10^{-2}$  and  $1 \times 10^{-2}$  respectively. These capillary numbers are much larger in comparison to the capillary number of water and milk. Because the capillary numbers for xanthan gum and sputum are slightly larger than the capillary number of water and milk, as seen from the results, both xanthan gum and artificial sputum require 5 more swipes and 10 more swipes respectively to fill the wells than water.

If capillary forces are greater than viscous forces, then the liquid is able to compartmentalize into the nanowells. However, if capillary forces are smaller than viscous forces, then the liquid will not compartmentalize into the nanowells and instead remain on the top surface.

#### **4.2 Distribution of bacteria**

The distribution of the bacterial cells within an array of nanowells was studied at different concentrations. Based on calculations, a concentration of  $10^6$  cells/mL, for



instance, equated to 1 bacterial cell per nanoliter. Thus, in order to test this hypothesis, an array of 1nL nanowells was prepared and tested the distribution of various concentrations of bacteria. The solution that was deposited within the wells, to determine distribution, was LB media mixed with bacteria. Eleven wells were sampled with a concentration of  $10^8$  cells/mL,  $10^6$  cells/mL, and  $10^4$  cells/mL, which were each, repeated 3 different times. According to experimental results, a concentration of  $10^8$  bacterial cells per mL, resulted in a mean distribution of 47.6 cells/mL (4.76% of the expected result) with a standard deviation of 10.4. According to calculations, a concentration of  $10^8$  cells/mL should have contained 1000 bacterial cells per well (1nL). The results obtained from the experiment are very different than that of the expected bacterial deposition per well. A concentration of  $10^6$  cells/mL resulted in a mean value of 4.5 bacterial cells per well and a standard deviation of 2.2. This value was similar to the expected value of 1 bacterial cell per well (1nL). Finally, at a concentration of  $10^4$  the bacterium was scattered and scarce, only to have 1 bacterium present in certain wells while others contained no bacterium at all. The mean distribution of a concentration of  $10^4$  cells/mL was found to be 1 cell in 6 (mean value) different nanowells among 100 nanowells (the remaining wells had no bacteria) with a standard deviation of 2.0. This was expected and close to the expected value, and in accordance to calculations: a concentration of  $10^4$  cells/mL should contain 0.01 cells/nL, which means that 1 bacterial cell will exist per 100 wells that won't have any bacteria.

### **4.3 Demonstration of metabolic monitoring of bacterial growth**

Oxygen quenching ruthenium dye was added to the bacterial solution in order to monitor the oxygen consumption of the bacteria as a direct measure of the presence, viability and drug susceptibility of bacteria. The bacterial solution was composed of GFP tagged E.coli K12 strain with a concentration of  $10^8$  cells/mL mixed with LB media and 0.3mg/mL of Ru(BPY)<sub>3</sub> ruthenium dye. The use of a microscope allowed the enumeration results of bacterial micro-colony counting as well as oxygen fluorescence measurements. Thus, a picture was taken using a confocal microscope to demonstrate the increase of fluorescent intensity over 2 hours. With the use of a confocal microscope, the presence of bacterium was allocated and then were able to simultaneously study the Ru(BPY)<sub>3</sub> fluorescence intensity changes in the wells that contained the bacterium, and disregarded the nanowells that contained no bacterium. As shown in figure 21, a 1 nL well volume with bacterial solution of  $10^8$  CFU/mL bacterial concentration with oxygen quenching dye, Ru(BPY)<sub>3</sub> was sealed in the well and taken to be imaged so that oxygen consumption levels could be visualized with the use of the confocal microscope. There is an evident and visual increase in the fluorescent intensity of the bacterial well in under two hours.

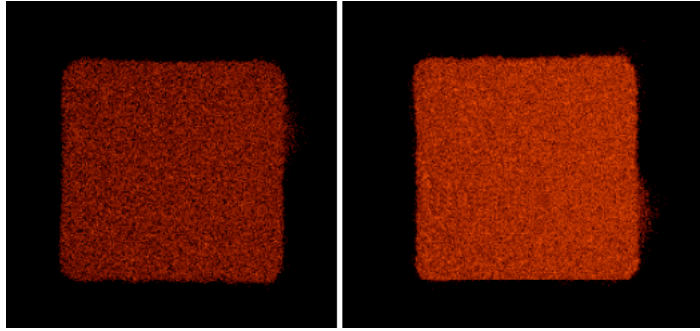


**Figure 21.** Confocal microscopy imaging was used to capture a 1 nL well volume. Fluorescence of the oxygen quenching fluorophore Ru(BPY)<sub>3</sub> is imaged. The image on the left is at time=30min and figure on the right is time=2 hrs at a concentration of 10<sup>9</sup>CFU/mL.

Calibration of the spectral fluorescent intensity was done as a reference to all other experiments presented in this chapter. The first test was obtained by dissolving the oxygen scavenger, Sodium Sulphite, in LB media and Ru(BPY)<sub>3</sub> to remove all the dissolved oxygen. Dissolved oxygen was measured using a standard meter (model YSI 550A, YSI Environmental, Yellow Springs, Ohio). This yielded a solution with an oxygen concentration of 0 mg/L. The second test was conducted by bubbling oxygen gas into our LB media solution, mixed with Ru(BPY)<sub>3</sub>, with an oxygen concentration of 15.6 mg/L, as a measure of maximum oxygen concentration within the nanowells. The purpose of using an oxygen scavenger (min; [O<sub>2</sub>] = 0 mg/L) and pure O<sub>2</sub> (max; [O<sub>2</sub>] = 15.6 mg/L) was to obtain results for the fluorescent intensity at maximum and minimum values (results not shown), as a reference for all the experiments that would be done following this (adjust the gain and amplitude offset accordingly). The last control was conducted

with LB media as it would have been obtained. Experimental data points were recorded every minute, over an hour for the controls in our experiment. They were also repeated three different times, and 14 wells were analyzed and processed in total. All fluorescent intensities observed in figure 22 were normalized to zero by  $x_t - x_0$  (as mentioned in materials and methods).

Sodium sulfite was used to remove oxygen completely from the LB media, which was then mixed with  $\text{Ru}(\text{BPY})_3$ . An oxygen measurement was taken once the sodium sulphite was added to the solution, and it was measured to be  $[\text{O}_2] = 0 \text{ mg/L}$ . This appeared as an extremely bright fluorescent signal under a confocal microscope. But it was soon evident that the fluorescent intensity began to decrease over time (55 minutes) as shows in figure 22 (represented by green triangles). This result was expected, as PDMS is gas permeable and there will be an expected gas exchange yet minimal as seen in the results (a decrease of nearly 4 units), with a 1.02% difference. PDMS has a diffusion coefficient of  $D_{\text{PDMS}} = 3.25 \times 10^{-9} \text{ m}^2/\text{s}$ . Thus, it is evident that the oxygen will naturally want to reach equilibrium and thus diffuse from a higher partial pressure of oxygen to a lower one. This can be demonstrated with Ficks law of diffusion.

$$J = -D \frac{\partial \phi}{\partial x} \quad (3)$$

$J$  is the "diffusion flux", which measures the amount of substance that flows through a unit area with a specific time interval,  $\text{mol m}^{-2} \text{s}^{-1}$ .  $D$  is the diffusion coefficient or diffusivity,  $\text{m}^2/\text{s}$ ,  $\phi$  (for ideal mixtures) is the concentration, units of  $\text{mol}/\text{m}^3$ ,  $x$  is position, the dimension of which is length

The partial pressure of oxygen in atmospheric air is 160 mm Hg, that is 20.95% of ambient air is made up of oxygen[71]. In comparison to the oxygen concentration in the sodium sulphite solution was 0mg/L, which corresponds to 0 mmHg. Since atmospheric pressure is higher than the dissolved oxygen concentration, diffusion will cause the oxygen to drift from the liquid to the atmosphere through the PDMS layer. This is the reasoning behind the decrease in fluorescent intensity over time (green triangles, figure 22). However, in the second case, when oxygen was bubbled into the solution, the dissolved oxygen concentration was 266.5mmHg. Since the atmospheric oxygen partial pressure is 160 mm Hg, through the law of diffusion, the oxygen will travel from the air into the solution. This can be seen in figure 22 (blue diamonds), when oxygen is bubbled into the solution, the oxygen escapes through the PDMS. Since the fluorophore is oxygen quenching, when the amount of oxygen decreases in the well, the fluorescent intensity

increases. That is exactly what is happening in the figure below. Thus, based on the diffusion law, oxygen will diffuse from the atmosphere into the nanowell device in order to achieve equilibrium. Because PDMS is a diffusive material, allows the exchange of gas, it is likely that oxygen from the ambient air was entering through the PDMS through diffusion.

In the second case, LB media mixed with Ru(BPY)<sub>3</sub> (0.3mg/mL) was bubbled with oxygen gas ([O<sub>2</sub>] = 15.6 mg/L), compartmentalized within the nanowells and sealed. This resulted in very dim fluorescent images under a fluorescent microscope, which slowly but gradually increased in fluorescent intensity over time (55minutes). As shown in figure 22, (represented by blue diamonds) the fluorescent intensity seemed to increase by of nearly 6 units. This too, like the case of the sodium sulphite was an expected result. Since PDMS is gas permeable it was very likely that the concentrated gas within the wells diffused out of the PDMS and into the ambient air (less concentrated oxygen) to try and attain equilibrium. However, once again the changes were very minimal, at 4.8% and almost insignificant. These experiments were also done in order to set the minimum and maximum fluorescent intensities.

Lastly, an experiment was conducted whereby Ru(BPY)<sub>3</sub> and LB media solution, under ambient conditions, was segmented into nanowells and taken to a confocal microscope for imaging. As shown in figure 22, there was a smaller change in

fluorescence intensity in comparison to the two other experiments (oxygen depleted and oxygen-saturated solutions). This was expected because gas exchange tends to be highest (or more likely) when there are uneven levels of oxygen within the wells versus the ambient air. Nevertheless, it seemed that with ambient conditions for the solution used, there was an evident increase (0.44% ) in fluorescent intensity, which signified that there was more oxygen diffusing out of the walls of the PDMS than there was entering. This could be used as a measure for later experiments (all experiments considered with bacteria are tested under ambient conditions), in which any increases as low as 2 units or smaller, could be considered as artifacts. This experiment was repeated three times, and studied and processed the fluorescence of a total of 21 nanowells.

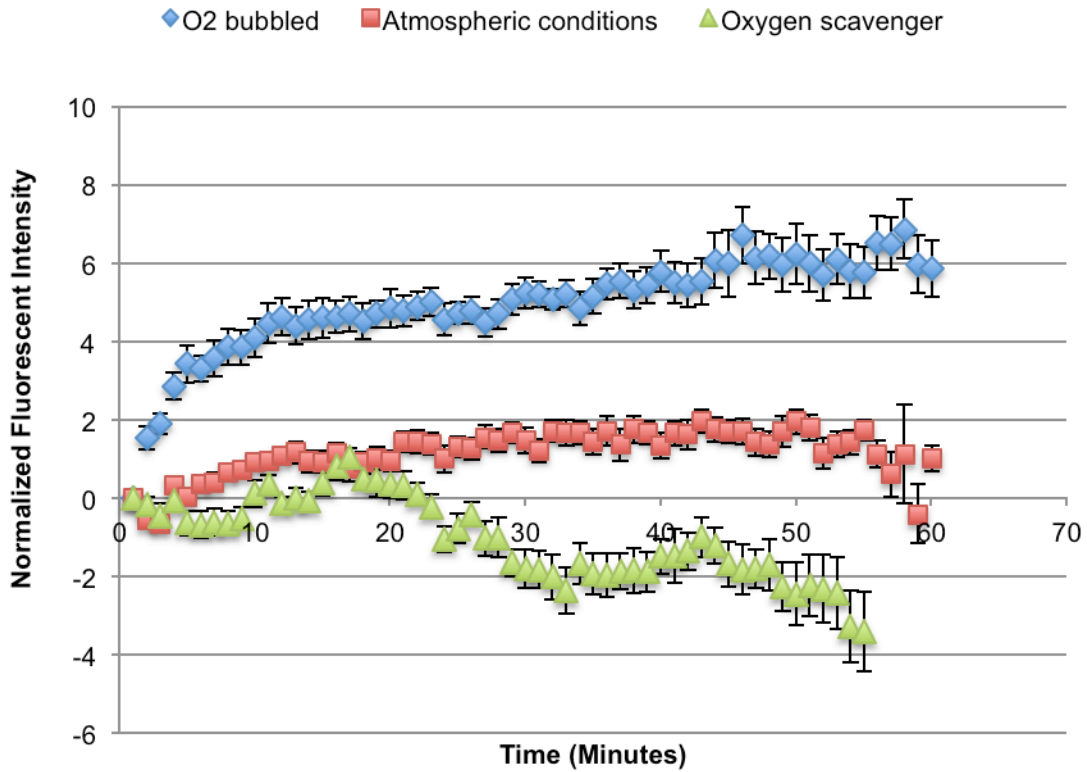


**Figure 22.** Controls. Fluorescence behavior when O<sub>2</sub> gas bubbled in solution ([O<sub>2</sub>] = 15.6 mg/l), at atmospheric conditions ([O<sub>2</sub>] = 6 mg/l), and when oxygen scavenger is added ([O<sub>2</sub>] = 0 mg/l) respectively. *Fluorescence intensities were normalized (to t=0) to allow direct comparison of fluorescent increases/decreases.*

#### 4.4 Bacterial Viability

Determining the bacterial viability is critical for assessing the presence of viable bacteria in contaminated samples and pathogenic samples, which can therein provide information on the antibiotic activity of the target sample [72], [73]. A viability study was performed that involved a long-duration incubation of GFP *E.coli* within the nanowell to



ensure bacterial growth and bacterial division in the microenvironment. In order to confirm this, a bacterial solution was prepared (refer to “bacterial culturing” in the materials and methods section) and mixed with 0.3 mg/mL of Ru(BPY)<sub>3</sub>. Bacterial solutions mixed with Ru(BPY)<sub>3</sub>, were encapsulated in the well made of PDMS. Initially there were several isolated bacteria present in the well as shown in figure 23 but bacterial growth increased over time, which was recorded 2.5 hours and then 5 hours later. Therefore, bacterial growth (division) increases with time within the nanowells, indicating bacterial viability. Since there is no disturbance in this particular microenvironment, the daughter cells were located right next to the mother cells and therefore forming in lines. Also, it was noted that after one day (24 hours) of incubation, the overgrown GFP-tagged *E.coli* became overpopulated in the well.

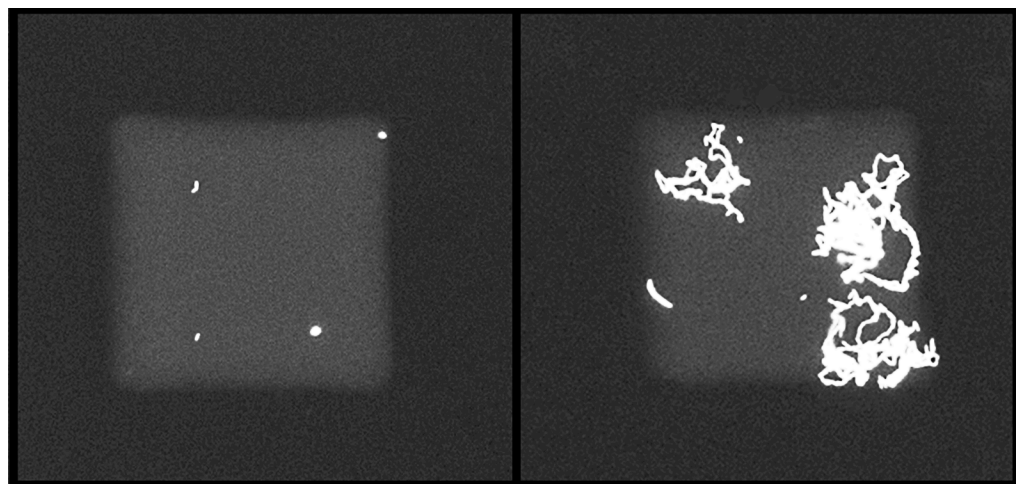


**Figure 23.** The growth of GFP-expressing *E. coli* K12 in LB media is demonstrated within a 1nL nanowell at image on left, t=0 and image on right, t=12hrs.

#### 4.5 Fluorescence response and bacterial metabolism

Fluorescent intensity corresponds to metabolic activity within the wells. The oxygen consumption rate of each *E.coli* bacterium is  $1.78 \times 10^{-18}$  mol/cell/s[74]. An experiment was set up so that a concentration of  $10^8$  cells/mL was mixed with LB media and 0.3mg/mL of Ru(BPY)<sub>3</sub>, sealed and imaged using a confocal microscope. Ru(BPY)<sub>3</sub> is oxygen quenching, so the fluorescent intensity increases with oxygen depletion within nanowells. A number of experiments were done in order to study whether the metabolic activity was directly related to cell viability.

This was demonstrated with different concentrations of bacteria. The higher concentrations of bacteria were expected to demonstrate higher bacterial metabolic activity (faster rates of oxygen consumption; faster fluorescent intensity increasing rates), as there are a greater number of viable cells. Meanwhile the lower concentration of bacteria should demonstrate lower metabolic changes, since there are fewer bacterial cells per well. As figure 24 illustrates that this in fact was the case. At the  $10^8$ ,  $10^6$ ,  $10^4$  CFU/mL, rates of fluorescent intensity changes were more drastic with higher concentration and lower rates of change with lower concentrations such as  $10^4$  CFU/mL. Therefore the level of fluorescent intensity is indicative to the number of active bacteria present. Each of these experiments was repeated 3 times and the average number of wells analyzed was 5 nanowells. With its high sensitivity, and low cytotoxicity, Ru(BPY)<sub>3</sub>

makes the ideal sensor for studying oxygen levels within the bacteria-containing wells. It is reported that RU(BPY)3 is able to reliably detect and differentiate between oxygen levels at a concentration of as little as  $8 \mu\text{M}$ [60], which is especially critical for our application.

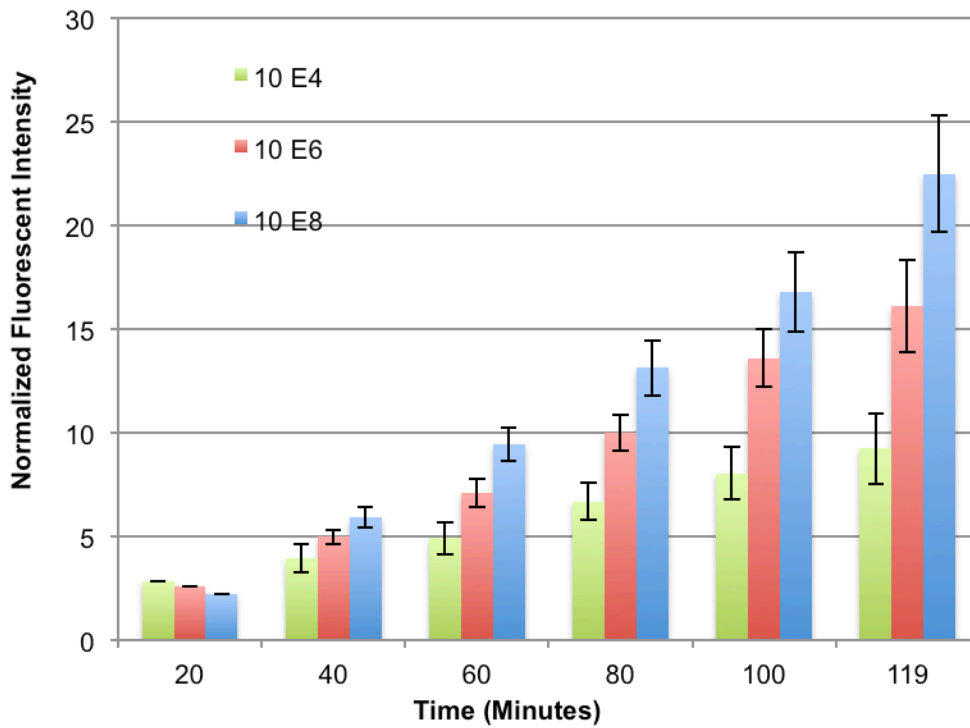


**Figure 24.** Different Concentrations of bacteria were imaged for metabolic rates of detection. Fluorescence intensities were normalized (to  $t=0$ ) to allow direct comparison of fluorescent increases.

## 4.6 Drug susceptibility

It is imperative to administer drugs and to rapidly appraise drug by obtaining quick results of the drug susceptibility of the bacteria[75]. This is also especially important for the prevention of drug resistant bacteria, which is becoming a major problem, which develops because of overtreatment[75]. By adding the appropriate drug to the broth and measuring metabolic changes of the bacteria with the use of RU(BPY)<sub>3</sub> as a measure of oxygen concentration levels is a critical factor for studying drug resistance. Fluorescent intensity corresponds to the bacterial metabolic activity, which is directly proportional to the number of living cells[76]. The purpose of this experiment was to use RU(BPY)<sub>3</sub> to test the effect the drug, ampicillin (AMP) had on the E coli OP50 strain. In the experiment, 100  $\mu\text{L}$  of ampicillin was added [77] into a bacterial broth with a concentration of  $10^6$  cells per mL to inhibit the cell growth. The results in figure 25 illustrates that by adding ampicillin into the solution, bacterial growth is inhibited, whereas, the wells that did not contain any ampicillin allowed for bacteria to culture as it naturally would, resulting in a fluorescence increase. Antibiotics like ampicillin act as an irreversible inhibitor of the enzyme transpeptidase, which is needed by the OP50 E.coli bacteria to make their cell walls, and ultimately stops lysis. If the bacteria are in fact sensitive to the drug, there should be no (or little) evident increase in fluorescent intensity, which signifies that there is no metabolic activity occurring. Damaged and dead

bacterial cells have lower innate metabolic activity[76], and thus will not consume oxygen. The oxygen quenching properties of Ru(BPY)<sub>3</sub> should show no significant increase in fluorescent intensity, which will signify that there is no oxygen uptake of the bacteria within the wells, which is a direct measure of drug sensitivity.

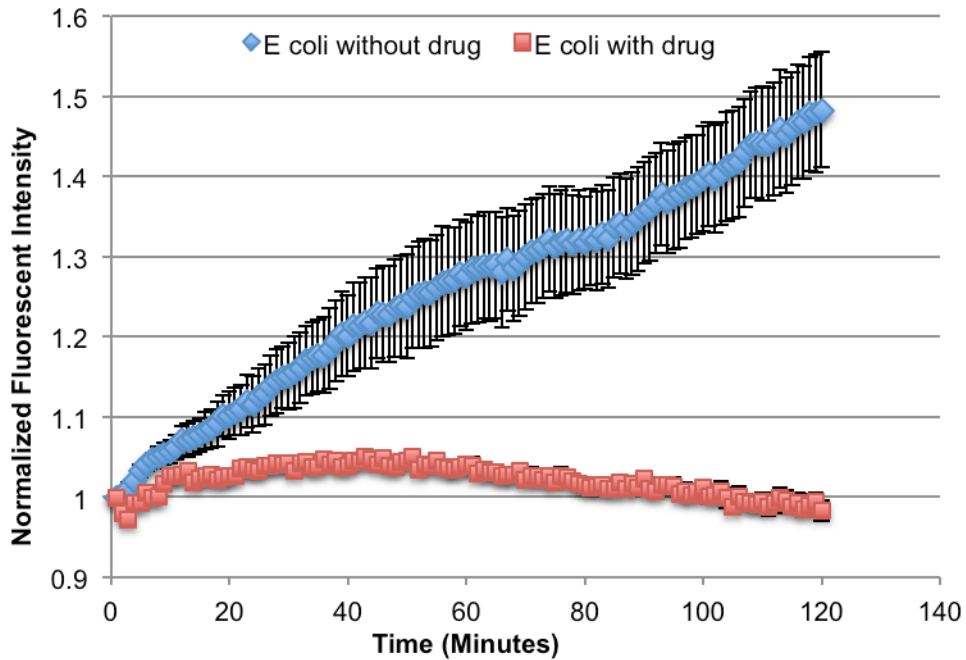


**Figure 25.** Confocal microscopy is used to image the fluorescent intensity of the Ru(BPY)<sub>3</sub> when a drug (ampicillin) is added to the nanowell, it inhibits bacterial growth, whereas when no drug is present in the well, the e coli OP50 strain grows naturally and it can be observed that an increase in fluorescence occurs due to oxygen quenching. *Fluorescence intensities were normalized (to t=1) to allow direct comparison of fluorescent increases/decreases.*

#### 4.7 Nanowell Shape and Size

Two geometries for the nanowell devices were fabricated, one consisted of an array of square wells, and the second was an array of circular wells. According to the results obtained, there is no difference between the two geometries on the results. According to a research group, the triangular shaped nanowells were a better fit for cell trapping, yet they also found that there was no difference found between square and circular shaped wells on the accuracy of bacterial cell trapping[78].

An experimental setup was then done in order to study the effect of the nanowell size (volume) on detection times. This was demonstrated by using an E coli (K12 strain) bacterial solution that is serially diluted to obtain a concentration of  $10^4$  cells/mL, mixed with LB media, and 0.3 mg/mL Ru(BPY)<sub>3</sub>. The bacterial concentration remained constant throughout this experiment, to study the effect of well size on detection times. Then, three various sized wells were selected: 0.1 mL, 100 nL and 1nL respectively. It was noted that the smaller sized nanowells allowed detection time to increase significantly at lower concentrations of bacteria. As demonstrated in figure 26 with smallest sized well (1nL volume), there was a substantial increase in fluorescent intensity in comparison to the 100nL volume which showed a slower rate of increase and 0.1mL which showed an relatively small increase over time. Each of these experiments was

repeated 3 times, and a total of 5 wells were studied and processed for the measurements of the 100 nL volume and the 0.1 mL volume.

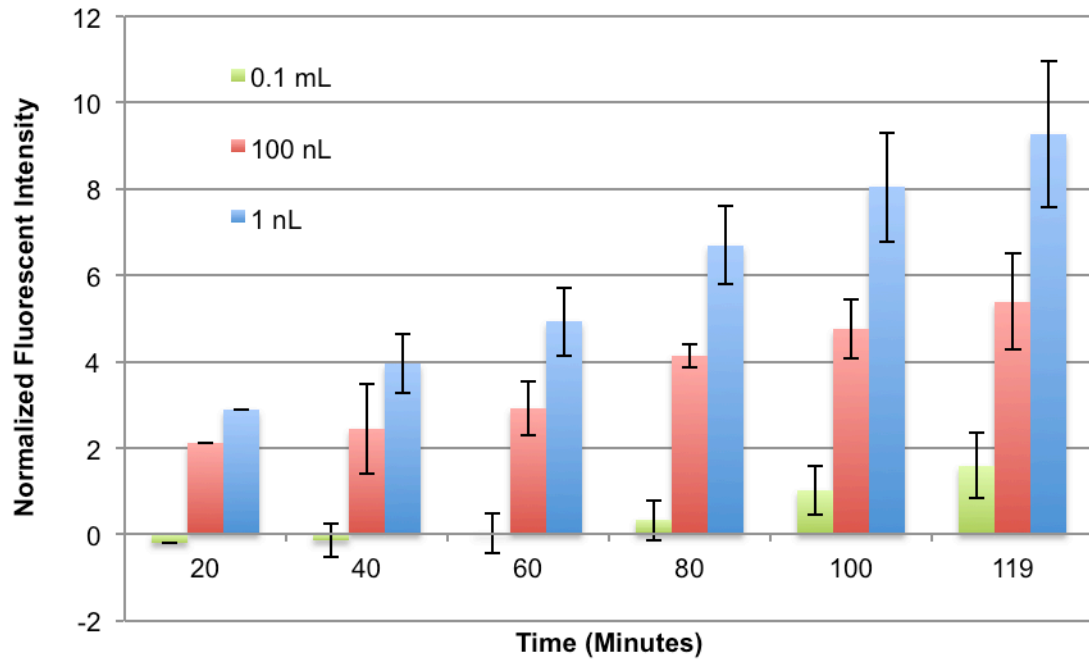


**Figure 26.** The volume size of the nanowell effects the results significantly. The smaller the well volume (100nL, 1nL), the more prominent the changes in oxygen levels within the well. The larger the well, the longer the time it takes to detect changes in oxygen levels (0.1mL). *Fluorescence intensities were normalized (to t=0) to allow direct comparison of fluorescent increases.*

## 4.8 Summary

In this chapter, bacterial diagnostics using a combination of oxygen quenching fluorophore along with nanovolumes was demonstrated to be a quick and effective method to detect bacteria. The experimental results with 3 types of samples (GFP tagged

bacteria, Bacteria with fluorophore and drug susceptibility) were illustrated and discussed. The effect of nanowell volume/spacing/size, concentration of bacteria, concentration of fluorophore was characterized. The results show that the nanowell device is able to detect bacterial presence and viability and drug susceptibility in 40minutes.



## **Chapter 5.**

# **Contributions and Future Work**

### **5.1 Contributions**

In an effort to improve the gold standard, culture test, instead of analyzing bacterial presence based on growth, to analyze it based on metabolic rates instead. These nanowell devices that have been fabricated have many potential applications for many industries (medical, food, etc), and to be able to test and study bacteria with rapid, accurate, and effective responses.

These results are important not only for the characterization of the detection device that is describe in this thesis but also for understanding the behavior of bacteria within the microenvironment. The relationship parallelization and miniaturization will increase oxygen consumption in bacteria especially at lower concentrations of bacteria. In this thesis, results show that metabolic rate was directly related to the oxygen consumption of the bacteria by testing the different concentrations of bacteria to ensure that the more living cells present within wells showed faster metabolic rates, in comparison to lower concentrations of bacteria which showed slower rates of metabolic

activity. The results also describe how the smallest size wells had the fastest rate of change over time, which hold great promise for drastically speeding turnaround times. Drug resistance is also able to be determined very clearly from test results. Therefore unlike the majority of bacterial detection methods that currently exist, the diagnostic approach proposed in this thesis, will be able to provide all information sought by healthcare professionals such as the bacterial presence, viability and drug-resistance quickly and effectively. Additionally, the detection method discussed in this thesis, is very easy to fabricate and operate, is a low-cost device, and most importantly will have fast turnaround times for results

Compared with the conventional diagnostic methods introduced in Chapter 2, the approach developed in this thesis has the potential for the detection of bacterial presence, viability and drug susceptibility even at concentrations as low as  $10^4$  cells/mL. The integration of an oxygen quenching fluorophore into a bacterial solution provided some very valuable information on the bacteria within the nanowell. The thesis presents the characterization of the technique to aliquot a larger volume of fluid into thousands of smaller volumes for the metabolic monitoring. Different nanowell sizes were tested ranging from sizes as big as 0.1mL down to 1nL volumes. It was demonstrated that faster detection can be obtained by reducing the volume size. It was also evident from results that bacteria was capable of proliferating within the nanowell environment, in which the

metabolic activity could be studied. Ranges of different bacterial concentrations were tested at:  $10^4$ ,  $10^6$ ,  $10^8$  cells/mL to study presence and viability of bacteria. Lastly, tests were done to determine whether an antibiotic was effective at inhibiting the growth of E.coli. It was found that when the antibiotic was effective, oxygen consumption of the bacteria came to a halt, which was indicative of cell death or growth inhibition.

As discussed in Chapter 3, the mold of the device was fabricated using photolithography, and soft-lithography. When sent for mass production, the unit cost of each device will be very low, making it affordable. Additionally, the PDMS that is used to create the nanowell array is cheap, and disposable.

However, the most valuable contribution to the work thus far is, decreasing turnaround times culture test because real-time quantification can be realized using the device in this thesis.

## **5.2 Future Work**

While preliminary experiments have shown the value and potential of the diagnostic device, more work is needed including:

- 1) Experiments thus far have been tested using E.coli. Since preliminary results obtained from Ecoli testing as a proof-of-concept on the nanowell device, this can then be applied on more pathogenic bacteria in the future, including M.bovis, and eventually tuberculosis

itself. Tuberculosis, for instance, is most prevalent in resource-poor settings, particularly third world countries. Thus, inexpensive devices that can quickly and effectively diagnose and treat the patient without the need for trained personnel are necessary.

2) Detection of Metabolism of bacteria. This thesis presented a solution to detect bacterial presence, viability and drug susceptibility using oxygen as an indicator of an active metabolism of the bacteria being tested, which directly correlates to the bacteria. However, in the future there could be many other metabolic tests that could be done to improve the specificity of the test by introducing biochemical fluorophores that can detect changes in pH for instance. An example of a bacterium that is suitable for this application is the *Helicobacter pylori*, as discussed in chapter 2.

3) A point of care testing (POCT) device is a requirement for this device. Conventional healthcare practice for diagnostics involves taking a sample and transporting it to a lab, whereby results would be returned after some time. This extends the turnaround times unnecessarily. Thus, by creating a portable diagnostic tool that can be at the time and place of the patient with real-time detection and results, the shorter the turnaround times become and as a result more lives can be saved. The development and design of a portable device that can automatically detect bacterial presence, viability and drug susceptibility will decrease turnaround times significantly, and patients can begin treatment almost immediately. The fluorescent microscope can be simplified with a LED light source, optical filters and a light detector.

4) So far, throughout the experiments, a confocal microscope has been used to complete experiments, however, other team members are making a conventional and portable camera/LED device for the detection of bacteria that requires low power.

5) Extension on the application of the device. Due to the potential usage of bacterial detection in other topics, this device can be applied to other purposes besides the detection of infectious disease. In the future, the device may serve as a diagnostic tool for the food, water, and medical industries. The expected contribution from this work to the scientific research community will be in multiple areas. Now that sufficient data has been gathered on the detection of molecular oxygen levels within nanowells as a direct indicator of the presence, viability, and drug susceptibility of *E. coli*. Future steps would be put towards making the nanowell device have a higher specificity fit to meet the biochemical characterizations of the metabolites produced by the bacteria of interest. The focus of our research is ultimately culturable pathogenic bacteria. In the healthcare sector, infectious diseases, due to pathogenic agents, are responsible for approximately 25% of physician visits. Future diagnostic tests should be tested with: *Vibrio cholera*, *Enterohemorrhagic Escherichia coli*, and *mycobacteria tuberculosis*. The detection device presented in this thesis will have applications not only in healthcare systems, but also in different industries such as food and agriculture, environmental monitoring and bio-defense.

In conclusion, the device presented in this thesis realizes real-time detection of bacterial presence, viability and drug susceptibility. The sample preparation, loading, sealing, imaging and fabrication of the nanowell array are very simple and easy process. Additionally, the nanowell array has many different applications it can be used in making, including healthcare, food industry and water safety.

In the future, more experiments need to be done using clinical bacterial infections. The ultimate goal is to develop the device into a fast, inexpensive, accurate and portable appliance for bacterial monitoring.

## Reference:

- [1] J. W.-F. Law, N.-S. Ab Mutalib, K.-G. Chan, and L.-H. Lee, “Rapid methods for the detection of foodborne bacterial pathogens: principles, applications, advantages and limitations,” *Front Microbiol*, vol. 5, Jan. 2015.
- [2] “WHO | The global burden of disease: 2004 update,” *WHO | The global burden of disease: 2004 update*. [Online]. Available: [http://www.who.int/healthinfo/global\\_burden\\_disease/2004\\_report\\_update/en/](http://www.who.int/healthinfo/global_burden_disease/2004_report_update/en/). [Accessed: 09-May-2015].
- [3] “Infectious Diseases | The CSIS Global Health Policy Center.” [Online]. Available: <http://www.smartglobalhealth.org/issues/entry/infectious-diseases>. [Accessed: 09-May-2015].
- [4] “WHO | Tuberculosis,” *WHO | Tuberculosis*. [Online]. Available: <http://www.who.int/mediacentre/factsheets/fs104/en/>. [Accessed: 09-May-2015].
- [5] H. H. Pachecker, *The Immigrant’s Universe*. Xlibris, 2010.
- [6] P. Chakrabarti, “Early, Easy, Inexpensive Diagnosis An Urgent Need for Global TB Control,” in *Frontiers in the Convergence of Bioscience and Information Technologies, 2007. FBIT 2007, 2007*, pp. 241–244.
- [7] “Global Health Risks.” [Online]. Available: [http://www.who.int/healthinfo/global\\_burden\\_disease/GlobalHealthRisks\\_report\\_part2.pdf](http://www.who.int/healthinfo/global_burden_disease/GlobalHealthRisks_report_part2.pdf). [Accessed: 21-Jul-2016].
- [8] R. I. Krasner, *The Microbial Challenge: Science, Disease and Public Health*. Jones & Bartlett Publishers, 2010.
- [9] “Antibiotic Resistance Threats in the United States, 2013 | Antibiotic/Antimicrobial Resistance | CDC.” [Online]. Available: <http://www.cdc.gov/drugresistance/threat-report-2013/>. [Accessed: 23-Aug-2016].
- [10] V. Nizet and J. D. Esko, “Bacterial and Viral Infections,” in *Essentials of Glycobiology*, 2nd ed., A. Varki, R. D. Cummings, J. D. Esko, H. H. Freeze, P. Stanley, C. R. Bertozzi, G. W. Hart, and M. E. Etzler, Eds. Cold Spring Harbor (NY): Cold Spring Harbor Laboratory Press, 2009.
- [11] L. J. Favor, *Eukaryotic and Prokaryotic Cell Structures: Understanding Cells with and Without a Nucleus*. The Rosen Publishing Group, 2005.
- [12] “Differences between Prokaryotes and Eukaryotes. | biochemanics.” [Online]. Available: <https://biochemanics.wordpress.com/2013/03/29/differences-between-prokaryotes-and-eukaryotes/>. [Accessed: 29-Jun-2016].
- [13] R. G. Krueger, N. W. Gillham, and J. H. Coggin, *Introduction to microbiology*. Macmillan, 1973.

- [14] K. C. Huang, R. Mukhopadhyay, B. Wen, Z. Gitai, and N. S. Wingreen, “Cell shape and cell-wall organization in Gram-negative bacteria,” *PNAS*, vol. 105, no. 49, pp. 19282–19287, Dec. 2008.
- [15] “Difference Between Gram Positive and Gram Negative Bacteria | Major Differences.” [Online]. Available: [http://www.majordifferences.com/2013/10/difference-gram-positive-vs-gram\\_2.html#.V7dElxPF\\_bB](http://www.majordifferences.com/2013/10/difference-gram-positive-vs-gram_2.html#.V7dElxPF_bB). [Accessed: 19-Aug-2016].
- [16] R. M. Atlas, *Instructor’s manual: Microbiology, fundamentals and applications, 2nd edition [by] Ronald M. Atlas*. New York; London: Collier Macmillan, 1988.
- [17] T. Akerlund, K. Nordström, and R. Bernander, “Analysis of cell size and DNA content in exponentially growing and stationary-phase batch cultures of *Escherichia coli*,” *J Bacteriol*, vol. 177, no. 23, pp. 6791–6797, Dec. 1995.
- [18] “Wiley: Microbiology - Dave Wessner, Christine Dupont, Trevor Charles.” [Online]. Available: <http://ca.wiley.com/WileyCDA/WileyTitle/productCd-EHEP002538.html>. [Accessed: 28-May-2015].
- [19] S. Chawla, “Carbon and nitrogen metabolism,” 2008.
- [20] O. Bonilla-Findji, J.-P. Gattuso, M.-D. Pizay, and M. G. Weinbauer, “Autotrophic and heterotrophic metabolism of microbial planktonic communities in an oligotrophic coastal marine ecosystem: seasonal dynamics and episodic events,” *Biogeosciences*, vol. 7, no. 11, pp. 3491–3503, Nov. 2010.
- [21] I. Schmidt, “Chemoorganoheterotrophic growth of *Nitrosomonas europaea* and *Nitrosomonas eutropha*,” *Curr. Microbiol.*, vol. 59, no. 2, pp. 130–138, Aug. 2009.
- [22] J. A. Washington, “Principles of Diagnosis,” in *Medical Microbiology*, 4th ed., S. Baron, Ed. Galveston (TX): University of Texas Medical Branch at Galveston, 1996.
- [23] R. Vasanthakumari, K. Jagannath, and S. Rajasekaran, “A cold staining method for acid-fast bacilli,” *Bull World Health Organ*, vol. 64, no. 5, pp. 741–743, 1986.
- [24] C. Lamanna, “The Nature of the Acid-fast Stain,” *J. Bacteriol.*, vol. 52, no. 1, pp. 99–103, Jul. 1946.
- [25] “Details - Public Health Image Library (PHIL).” [Online]. Available: <http://phil.cdc.gov/phil/details.asp?pid=5789>. [Accessed: 31-Aug-2016].
- [26] Y. Cheng, H. Xie, P. Sule, H. Hassounah, E. A. Graviss, Y. Kong, J. D. Cirillo, and J. Rao, “Fluorogenic Probes with Substitutions at the 2 and 7 Positions of Cephalosporin are Highly BlaC-Specific for Rapid Mycobacterium tuberculosis Detection,” *Angew. Chem. Int. Ed.*, vol. 53, no. 35, pp. 9360–9364, Aug. 2014.
- [27] K. Chawla, S. Gupta, C. Mukhopadhyay, P. S. Rao, and S. S. Bhat, “PCR for *M. tuberculosis* in tissue samples,” *The Journal of Infection in Developing Countries*, vol. 3, no. 02, Mar. 2009.



- [28] K.-W. Min, J. Y. Ko, and C. K. Park, “Histopathological spectrum of cutaneous tuberculosis and non-tuberculous mycobacterial infections,” *Journal of Cutaneous Pathology*, vol. 39, no. 6, pp. 582–595, Jun. 2012.
- [29] de L. Gw, B. Rg, S. Sm, and O. Dj, “Tuberculosis in free-ranging wildlife: detection, diagnosis and management.,” *Rev Sci Tech*, vol. 21, no. 2, pp. 317–334, Aug. 2002.
- [30] H. M. Lappin-Scott and J. W. Costerton, *Microbial Biofilms*. Cambridge University Press, 2003.
- [31] J. Modric, “Lab Tests for Staph | Healthhype.com.” .
- [32] P. L. Dolan, J. C. Harper, and S. M. Brozik, “Microbial Detection Systems,” in *Encyclopedia of Medical Devices and Instrumentation*, John Wiley & Sons, Inc., 2006.
- [33] J. G. Bergey, &#32;John G. Bergey, &#32;Noel R. Holt, and &#32;Peter H. A. S. Krieg, *Bergey’s Manual of Determinative Bacteriology, 9th ed.* Lippincott Williams & Wilkins, 1994.
- [34] S. H. Cho, S. Warit, B. Wan, C. H. Hwang, G. F. Pauli, and S. G. Franzblau, “Low-Oxygen-Recovery Assay for High-Throughput Screening of Compounds against Nonreplicating Mycobacterium tuberculosis,” *Antimicrob. Agents Chemother.*, vol. 51, no. 4, pp. 1380–1385, Apr. 2007.
- [35] W. L. Irving, D. Ala’Aldeen, and T. Boswell, *Medical Microbiology*. .
- [36] J. B. Sinclair and O. D. Dhingra, *Basic Plant Pathology Methods*. CRC Press, 1995.
- [37] *Methods in Microbiology*. Academic Press, 1987.
- [38] S. C. Edberg, F. Ludwig, and D. B. Smith, *The Colilert System for Total Coliforms and Escherichia Coli*. AWWA Research Foundation, 1991.
- [39] M. Cheesbrough, *District Laboratory Practice in Tropical Countries*. Cambridge University Press, 2006.
- [40] “NOAA Ocean Explorer: Estuary to the Abyss.” [Online]. Available: <http://oceanexplorer.noaa.gov/explorations/04etta/background/antimicrobial/media/antimicrobial2.html>. [Accessed: 31-Aug-2016].
- [41] P. G. Engelkirk and J. L. Duben-Engelkirk, *Laboratory Diagnosis of Infectious Diseases: Essentials of Diagnostic Microbiology*. Lippincott Williams & Wilkins, 2008.
- [42] “MIC DETERMINATION BY MICROTITRE BROTH DILUTION METHOD.” [Online]. Available: <http://cmdr.ubc.ca/bobh/methods/MICDETERMINATIONBYMICROTITREBROTHDILUTIONMETHOD.htm>. [Accessed: 31-Aug-2016].
- [43] Y.-W. Tang, G. W. Procop, and D. H. Persing, “Molecular diagnostics of infectious diseases,” *Clinical Chemistry*, vol. 43, no. 11, pp. 2021–2038, Nov. 1997.

- [44] K. S. Gracias and J. L. McKillip, “A review of conventional detection and enumeration methods for pathogenic bacteria in food,” *Can. J. Microbiol.*, vol. 50, no. 11, pp. 883–890, Nov. 2004.
- [45] A. McKie, A. Vyse, and C. Maple, “Novel methods for the detection of microbial antibodies in oral fluid,” *The Lancet Infectious Diseases*, vol. 2, no. 1, pp. 18–24, Jan. 2002.
- [46] Mohanty, *TB of Immunology*. Jaypee Brothers Publishers, 2010.
- [47] “Overview of ELISA.” [Online]. Available: <http://www.piercenet.com/method/overview-elisa>. [Accessed: 28-May-2015].
- [48] L. M. Parsons, Á. Somoskövi, C. Gutierrez, E. Lee, C. N. Paramasivan, A. Abimiku, S. Spector, G. Roscigno, and J. Nkengasong, “Laboratory Diagnosis of Tuberculosis in Resource-Poor Countries: Challenges and Opportunities,” *Clin Microbiol Rev*, vol. 24, no. 2, pp. 314–350, Apr. 2011.
- [49] E. S. Oh, M. M. Mielke, P. B. Rosenberg, A. Jain, N. S. Fedarko, C. G. Lyketsos, and P. D. Mehta, “Comparison of Conventional ELISA with Electrochemiluminescence Technology for Detection of Amyloid- $\beta$  in Plasma,” *J Alzheimers Dis*, vol. 21, no. 3, pp. 769–773, 2010.
- [50] Y. Yamamoto, “PCR in Diagnosis of Infection: Detection of Bacteria in Cerebrospinal Fluids,” *Clin Diagn Lab Immunol*, vol. 9, no. 3, pp. 508–514, May 2002.
- [51] “Foundation Volume 2, Chapter 40b. Molecular Diagnostics of Ocular Infectious Disease: Polymerase Chain Reaction Diagnostics of Ophthalmic Disease.” [Online]. Available: <http://www.oculist.net/downat0502/prof/ebook/duanes/pages/v8/v8c040b.html>. [Accessed: 22-Aug-2016].
- [52] J. Maurer, *PCR Methods in Foods*. Springer Science & Business Media, 2006.
- [53] L. M. L. Nollet and F. Toldr?, *Advances in Food Diagnostics*. John Wiley & Sons, 2008.
- [54] Z. Liron, A. Bromberg, and M. Fisher, *Novel Approaches in Biosensors and Rapid Diagnostic Assays*. Springer Science & Business Media, 2012.
- [55] C. King and F. M. Henretig, *Textbook of Pediatric Emergency Procedures*. Lippincott Williams & Wilkins, 2008.
- [56] W. L. George, V. L. Sutter, D. Citron, and S. M. Finegold, “Selective and differential medium for isolation of *Clostridium difficile*,” *J Clin Microbiol*, vol. 9, no. 2, pp. 214–219, Feb. 1979.
- [57] E. H. Conradie and D. F. Moore, “SU-8 thick photoresist processing as a functional material for MEMS applications,” *J. Micromech. Microeng.*, vol. 12, no. 4, p. 368, 2002.

- [58] G. M. Whitesides, “The origins and the future of microfluidics,” *Nature*, vol. 442, no. 7101, pp. 368–373, Jul. 2006.
- [59] B.-H. Jo, L. M. Van Lerberghe, K. M. Motsegood, and D. J. Beebe, “Three-dimensional micro-channel fabrication in polydimethylsiloxane (PDMS) elastomer,” *Journal of Microelectromechanical Systems*, vol. 9, no. 1, pp. 76–81, Mar. 2000.
- [60] L. Birch, C. E. Dawson, J. H. Cornett, and J. T. Keer, “A comparison of nucleic acid amplification techniques for the assessment of bacterial viability,” *Lett. Appl. Microbiol.*, vol. 33, no. 4, pp. 296–301, Oct. 2001.
- [61] H. Yamada, S. Mitarai, L. Aguilan, H. Matsumoto, and A. Fujiki, “Preparation of mycobacteria-containing artificial sputum for TB panel testing and microscopy of sputum smears,” *Int. J. Tuberc. Lung Dis.*, vol. 10, no. 8, pp. 899–905, Aug. 2006.
- [62] “Methyl cellulose; 0262- Product Information Sheet.,” *Sigma-Aldrich | Methyl cellulose; 0262- Product Information Sheet*. [Online]. Available: <http://www.sigmaaldrich.com/catalog/product/sial/m0262?lang=en&region=CA>.
- [63] M. T. Lopez-Vidriero, J. Charman, E. Keal, D. J. De Silva, and L. Reid, “Sputum viscosity: correlation with chemical and clinical features in chronic bronchitis,” *Thorax*, vol. 28, no. 4, pp. 401–408, Jul. 1973.
- [64] F. J. de Bruijn, *Handbook of Molecular Microbial Ecology II: Metagenomics in Different Habitats*. John Wiley & Sons, 2011.
- [65] Y. Wang, D. Lee, L. Zhang, H. Jeon, J. E. Mendoza-Elias, T. A. Harvat, S. Z. Hassan, A. Zhou, D. T. Eddington, and J. Oberholzer, “Systematic Prevention of Bubble Formation and Accumulation for Long-Term Culture of Pancreatic Islet Cells in Microfluidic Device,” *Biomed Microdevices*, vol. 14, no. 2, pp. 419–426, Apr. 2012.
- [66] L. C. Taylor and D. R. Walt, “Application of High-Density Optical Microwell Arrays in a Live-Cell Biosensing System,” *Analytical Biochemistry*, vol. 278, no. 2, pp. 132–142, Feb. 2000.
- [67] S. R. Wickramasinghe, C. M. Kahr, and B. Han, “Mass transfer in blood oxygenators using blood analogue fluids,” *Biotechnol. Prog.*, vol. 18, no. 4, pp. 867–873, Aug. 2002.
- [68] G. Sworn, E. Kerdavid, P. Chevallereau, and J. FAYOS, “Improved xanthan gum,” EP2413714 A1, 08-Feb-2012.
- [69] S. Badilescu and M. Packirisamy, *BioMEMS: Science and Engineering Perspectives*. CRC Press, 2016.
- [70] R. O. Baker, H. W. Yarranton, and J. Jensen, *Practical Reservoir Engineering and Characterization*. Gulf Professional Publishing, 2015.
- [71] M. Losen, B. Frolich, M. Pohl, and J. Buchs, “Effect of Oxygen Limitation and Medium Composition on Escherichia coli Fermentation in Shake-Flask Cultures.” [Online]. Available: <http://www.hitec->

- zang.de/fileadmin/informationsmaterial/publikation/2004-05\_BP\_Losen\_Buechs.pdf. [Accessed: 17-Aug-2016].
- [72] R. J. Jackman, D. C. Duffy, E. Ostuni, N. D. Willmore, and G. M. Whitesides, “Fabricating large arrays of microwells with arbitrary dimensions and filling them using discontinuous dewetting,” *Anal. Chem.*, vol. 70, no. 11, pp. 2280–2287, Jun. 1998.
- [73] P. C. Thomas, L. E. Locascio, S. R. Ragahavan, and S. P. Forry, “ON-CHIP PERVERAPORATION-FREE CONTROL OF GAS PARTIAL PRESSURES,” National Institute of Standards and Technology, USA and University of Maryland, USA.
- [74] C. H. Chen, Y. Lu, M. L. Y. Sin, K. E. Mach, D. D. Zhang, V. Gau, J. C. Liao, and P. K. Wong, “Rapid Antimicrobial Susceptibility Testing Using High Surface-to-Volume Ratio Microchannels,” *Anal Chem*, vol. 82, no. 3, p. 1012, Feb. 2010.
- [75] J. T. Keer and L. Birch, “Molecular methods for the assessment of bacterial viability,” *J. Microbiol. Methods*, vol. 53, no. 2, pp. 175–183, May 2003.
- [76] D. Sud, “Wide-Field Time-Domain Fluorescence Lifetime Imaging Microscopy (FLIM): Molecular Snapshots of Metabolic Function in Biological Systems.,” 2008.
- [77] I. P. Thonus, P. Fontijne, and M. F. Michel, “Ampicillin susceptibility and ampicillin-induced killing rate of *Escherichia coli*.,” *Antimicrob Agents Chemother*, vol. 22, no. 3, pp. 386–390, Sep. 1982.
- [78] M. Urdea, L. A. Penny, S. S. Olmsted, M. Y. Giovanni, P. Kaspar, A. Shepherd, P. Wilson, C. A. Dahl, S. Buchsbaum, G. Moeller, and D. C. Hay Burgess, “Requirements for high impact diagnostics in the developing world,” *Nature*, vol. 444, pp. 73–79, Nov. 2006.

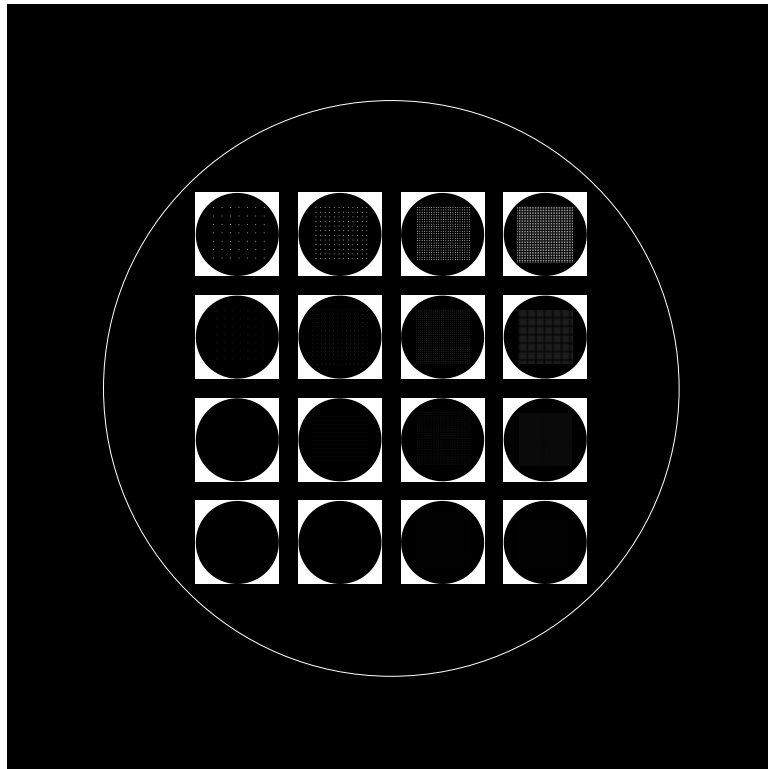
## Appendix A:

### Device Fabrication

The device were fabricated and assembled following these steps:

#### 1. Mask Preparation

1.1 Design channel features and dimensions using *inventor* as shown below.



**Mask for mold fabrication**

1.2 Send the file for mask printing.

## **2. Channel Mold Fabrication in Clean Room**

- 2.1 Immerse a silicon wafer in Acetone (1min), Methanol (1min), and DI water (5min) in order.
- 2.2 Place the wafer on hot plate of 150°C for 2 minutes.
- 2.3 Expose the wafer to oxygen plasma at 50 Watts for 30 seconds.
- 2.4 Place the wafer at the center of the spinner chuck.
- 2.5 Spin for sample mold (~100µm): pour about 3ml SU-8 100 photoresist at the center of the wafer; start spinning at 500 rpm for 5-10 sec with acceleration of 100 rpm/sec; increase the speed up to 4000 rpm with an acceleration of 1000 rpm/s, and continue for 30 sec at the final speed.
- 2.6 Move the wafer from spinner to a hot plate for soft bake.
- 2.7 Soft bake for sample mold: keep the wafer on a hot plate at 65°C for 10min and 95°C for 30min. If wrinkles on the photoresist appear during soft bake, remove the wafer from the hot plate, and put it back after the wrinkles gone.
- 2.8 Mount the mask on the mask aligner.
- 2.9 Align the mask and the wafer, and attach them when alignment is done.
- 2.10 Exposure for sample nanowell mold: expose the wafer to UV light through the mask for total exposure energy of 160mJ/cm<sup>2</sup>.
- 2.11 Move the wafer from mask aligner to a hot plate for post bake.

2.12 Post bake for sample mold: keep the wafer on a hot plate at 65°C for 1min and 95°C for 10min.

2.13 Immerse the wafer into SU-8 developer solution and occasionally stir until the features are clear (10 minutes).

2.14 Rinse the wafer with Isopropyl Alcohol (IPA).

2.15 Re-immerses the wafer back in developer solution if white residual appears.

2.16 Rinse with DI water, and dry with nitrogen.

2.17 Hard bake the wafer on hot place at 150°C for 30min.

### **3. PDMS Nanowell array Replica**

3.1 Place the wafer into a petri dish.

3.2 Mix 10:1 (base: curing agent) PDMS in a beaker by thoroughly stirring.

3.3 Pour around 20ml PDMS into each petri dish.

3.4 Place petri dishes in the oven at 60°C for 3hours.

3.5 Peel PDMS substrates off the mold, and cut it into appropriate pieces.

## **Appendix B:**

### **Measuring Mean Grey Value**

The fluorescence of nanowells can be measured using ImageJ using the following steps:

1. Select the nanowell of interest using the appropriate drawing tool (i.e. square, circle)
2. From the Analyze menu select “set measurements”. Make sure you have AREA, and MEAN GREY VALUE selected.
3. Next, select “Measure” from the analyze menu. You should now see a popup box with a stack of mean grey values for that first nanowell.

## **Appendix C:**

### **Inoculation of a Petri dish containing agar**

1. Prepare glass test tube with 4mL LB media and add appropriate antibiotic
2. Use sterile pipette tip to pick a single colony of bacteria
3. Drop the tip into LB media and antibiotic mixture



4. Cover the test tube with a loose cap to allow air exchange
5. Incubate bacterial culture at 37degrees for 12-14 hours in a shaking incubator
6. After incubation, check culture for growth (if clouded growth occurred).
7. Measure optical density O.D.<sub>600</sub> using a spectrophotometer to ensure concentration of bacteria is the same and consistent for all experiments.